# NUMERICAL OPTIMIZATION OF ION TRANSPORT IN ELECTROSPRAY MASS SPECTROMETRY

by

Kevin Rozmiarek

A thesis submitted to the Faculty and the Board of Trustees of the Colorado School of Mines in partial fulfillment of the requirements for the degree of Masters of Science (Applied Physics).

Golden, Colorado

Date _____

Signed: _____
Kevin S. Rozmiarek

Signed: _____
Dr. Timothy R. Ohno
Thesis Advisor

Golden, Colorado

Date _____

Signed: _____
Jeff A. Squier
Professor and Head
Department of Physics

ABSTRACT

Electrospray ionization (ESI) has developed into a key component of investigative analyses of samples in numerous biological, chemical, and geological contexts due to its unique ability to preserve the structure of ionized species without fragmentation. It is thus important that we fully understand and characterize the processes in order to correctly utilize its advantages. Proposed studies have called for the use of electrospray ionization to investigate trace species in mining runoff water as well as later studies of stable isotopes that are often inherently trace.

In this thesis I present a first attempt at modeling the ESI process in ion optics software SIMION. Two electrode geometries under consideration for use in these studies are presented to test if current understanding in literature is enough to construct simulations to support informed decision making on instrumentation. These geometries are an off-axis sample input and ”shadow block” lens. It is concluded that current literature is insufficient in any realistic systems as multiple assumptions must be made that limit the scope of this analysis. Discussion into these assumptions are presented as well as potential contexts where simulation is successful at the current stage in this field.

# TABLE OF CONTENTS

# LIST OF FIGURES

# ACKNOWLEDGEMENTS

I would like thank many people whose support made this research and thesis something I can be proud of.

First and foremost I would like to thank my parents, Ed and Susan, for their tireless dedication towards me and my success academically. They both serve as my role models for both work ethic and pride in quality of work which I hope they find here.

I would also like to thank those at the U.S. Geological Survey for their guidance and support while I do this research. Their financial support and interest in the results of this project is part of what made it possible.

I want to take time to thank my numerous friends and my girlfriend Katie for creating an environment in which we all can succeed in our academic endeavors. The tireless enthusiasm for science and our own work taught me that I wasn't the only crazy one. Thank you for that.

Finally, I would like to thank my colleague and advisor Dr. Ohno. Without his willingness to pick me up as a graduate student and his continuing guidance, this project wouldn't have gone anywhere in the first place.

# CHAPTER 1: INTRODUCTION AND BACKGROUND

In collaboration with the U.S. Geological Survey Crustal Geochemistry and Geophysics Stable Isotope Labs, it was deemed advantageous to provide an analysis and simulation of a new electrospray ionization source that is to be acquired in our continued effort to increase our ability to investigate trace species and stable isotopes across a broadband of geochemical and biological contexts. The sensitivity requirements and delicacy of measurements needed for chemical analysis of trace species implies that careful manipulation of ion optics and lensing leading ions to mass-spectrometers is of particular importance. In this thesis a simulation of the electrospray process is presented as well as its use in simple geometries to demonstrate the potential improvements that can be achieved with intelligently designed lensing setups.

## 1.1 Intended Studies

While an electrospray ionization source can be used in many different applications, the USGS has a few studies already in mind. The ability to preserve species structure during ionization (a feature that will be discussed later) can be key to the investigation of trace particulates in ”messy” signals. USGS intends to use this feature to investigate the propagation of cyanide and arsenic in water runoff from copper-gold mining operations in the western United States.

Many of gold’s features become annoyances when attempting to extract from low-yield ore. It possesses an inherent resistance to oxidation even when exposed to high heat and atmospheric air [1]. It also has a low redox potential, even for a transition metal [2]. These properties call for the necessity of cyanidation, the process of creating a coordination complex of gold with cyano-group complexes to create a solution in which gold can later be extracted. The currently accepted dissolution reaction for this process is show below in Eq. 1.1 [3].

$$2\mathrm{Au} + 4\mathrm{NaCN} + 2\mathrm{H_2O} + \mathrm{O_2} = 2\mathrm{NaAu(CN)_2} + 2\mathrm{NaOH} + \mathrm{H_2O_2} \tag{1.1}$$

The process in order to create the desired gold-cyanide coordination complex also produces a significant amount of chemical waste. Key among these are arsenic, zinc, copper, and free

cyanide. Current regulation allows for the pooling of waste materials on mining land in open pits. These open pits, seen in Fig. 1.1, are notoriously subject to weathering and runoff into nearby wildlife habitations, resulting in the death of smaller mammals and birds (where dosages of cyanide can reach lethal amounts) [4]. This fact, coupled with the reputation of the negative effects of arsenic on human health, has prompted the continuing study of runoff water from mining sites. Unfortunately, it may be difficult to identify the CN compound and its associated complexes in water without careful sample prep. Also, the high nucleophilicity of cyanide easily produces organic compounds characterized by their displaced halide group by cyanide. Called ”nitriles”, the formation of these compounds might indicate further contamination of ground water worthy of study. We hope to use the structure-preserving abilities of the electrospray along with its ability to have samples introduced in solution to study these chemical species as well as other cyano-group based compounds present in this runoff water.

Figure 1.1: An aerial view of the Mulatos Gold Mine in Sonora Mexico. The hydrogen-cyanide pits are distinguishable by their characteristic green hue of resulting copper oxides [5]

The addition of an electrospray to the arsenal of USGS’s stable isotope lab’s mass spectrometry systems is considerably valuable to investigate this runoff. As has just been stated, the

goal of studies in which this device is to be used is to detect trace amounts of substances and determine isotope signatures of geochemical processes and as such, accuracy is of the utmost importance. The ability to enable the largest amount of particles to reach the end of the lensing geometry and mass spectrometer directly relates to the error of the measurement as well as setting the resolution in which we start to see the separation in the representation of the isotopes.

In order for a mass spectrometer to take a measurement of quantitative accuracy, it will integrate a peak of signal from a Faraday cup. The integrated amount of an isotope is then compared to the integrated amount of another isotope establishing the isotopic ratio between the two. The peak is determined numerically from a derivative condition. As such, peak sharpness is a necessity when ensuring signal accuracy. It is this, coupled with the need for a large amount of particles to reach the end of the lensing geometry, that indicates that an investigator ought to consider how ions can successfully make it to the mass spectrometer.

A further motivating factor that encourages sensitivity is the case where a sample's isotope ratio is dependent on a spatial component of that sample. This implies that the ability to perform successful analysis with less sample corresponds with spatial resolution of that sample. In order to perform an experiment along these lines, not only would one need sensitivity to see a statistically significant difference in isotope ratio, they would also need to be able to minimize the sample needed so smaller and smaller pieces of the original sample can be taken. Regardless, the sensitivity is always the upper bound on the range of analyses that a system can perform and thus a priority for investigation.

The first natural step to ensure that particles make it where they are desired is to simulate particle trajectories and develop a lens structure and geometry. This ion optics consideration is commonly used as an analysis tool in the development of mass spectrometers but in the case of electrosprays, an investigator would encounter a major issue: the mass of the charged particle changes. The Coulombic fission events that happen throughout the droplets lifetime warrants the need to effectively simulate the process if instrumentation is ever going to achieve a reliable and optimized lens geometry.

With that in mind the development of a software package in Lua to work with the ion optics program SIMION was determined to be an initial first step. The current methodology in

electrospray ionization is to send enough sample through the line that it reaches the end of a mass spectrometer with a conventional lensing geometry. The need for the ability to detect trace molecules and investigate stable isotopes will require a more careful consideration however.

## 1.2 Stable Isotope Analysis

The context for which an electrospray is to be used is in stable isotope analysis. In conventional mass-spectrometer analysis, the identification of an unknown is generally the subject of investigation but not in stable isotope analysis. When analysis gets down to certain sensitivities, the slight difference in mass of different isotopes can be seen by a mass spectrometer. This creates a ratio of isotopes for a sample for an element of consideration. This is denoted $\delta^x$ of the lesser common isotope, x, to the more common isotope [6]. A widely known method that utilizes this is carbon dating (or any other radio-dating for that matter). Carbon dating investigates the ratio between the radioactive isotope of carbon, $^{14}C$, and its most common isotope, $^{12}C$ [7].

Radioactive decays are just one methodology that may cause a difference in isotope representation of an element to develop. There are many. These simple differences in mass can result from any statistical process that is affected by mass. This could be some chemical process, osmosis, or even gravity [8]. An example in the case of gravity is that one could determine the altitude that water came from by the isotopes of oxygen present in an $H_2O$ molecule. The heavier isotope, $^{16}O$, is simply found at lower altitudes [9].

It is difficult to determine where to look for a new representation of isotope differences at work. Because these differences can be so small, different elements have different regimes where an isotope difference can be observed [6]. Even after this, attaching the ratio to some aspect of the process leading to it can be tricky. Nevertheless, the list of usable elements for this method is constantly expanding and there is now a useful library of processes that can be linked to ratios within geochemical processes. These are the ones of interest to the USGS and with the introduction of the electrospray, we can utilize its unique abilities for our benefit.

## 1.3 The Electrospray

Since its humble beginnings in the 1980s, the method of electrospray ionization mass-spectrometry (ESMS) has developed into a methodology used by thousands of groups around the world. The electrospray ionization source has allowed for the expansion into the analyses of high molecular weight compounds of nearly all varieties rendering it invaluable in numerous chemical contexts [10]. It is thus important that, from a technical perspective, we are careful to understand and utilize this method to the greatest of its ability. A example electrospray in action can be seen below in Fig. 1.2.

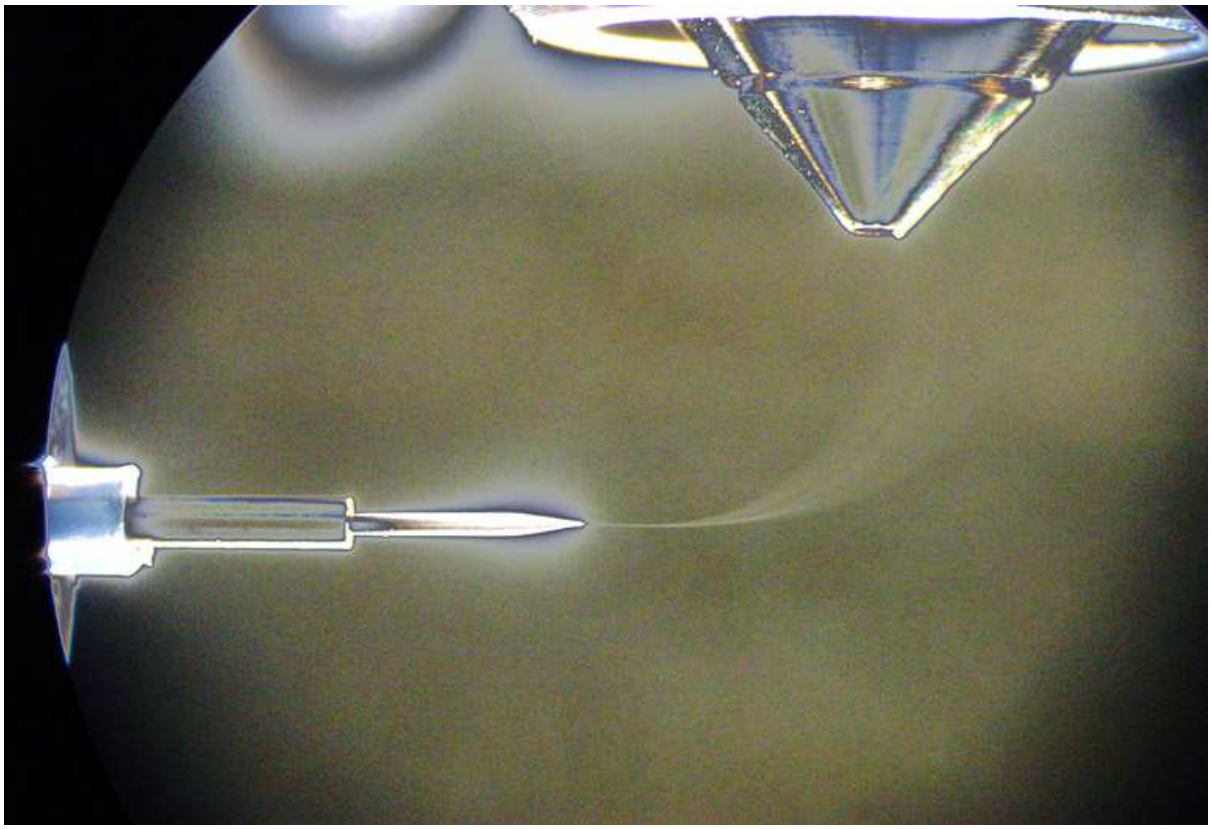

Figure 1.2: A contrast and brightness adjusted picture of an electrospray in action [11]

The electrospray offers many different and unique advantages. First and foremost is the idea that the electrospray is a "soft" ionization technique. That is to say that, unless forced, the resulting ionized gas does not contain any fragments of the original species [10]. Conventional methods of ionization must operate with energies that are sufficiently high to ionize the entire molecule yet those energies are almost always higher than one or more of the bonds within the atomic structure. An easy example of this apparent problem is the C-C bond. Any molecule

with a C-C bond has a total ionization energy above that of the $3.60eV$ it takes to break the bond [12]. This makes it difficult to perform an investigative analysis on simple organic molecules at best and impossible with any more complexity.

Another unique ability of the electrospray is to easily produce extensively multiply charged ions [10]. The increase in charge-to-mass ratio in these systems allows for compatibility with many different mass spectrometer setups that lack the ability to investigate higher mass ranges and also increases the apparent radius for collisions *in-vacuum* [13]. This gives us options to fragment the molecule post ionization, a fact that is the basis for tandem mass-spectrometry (MS/MS), the method that was awarded the Nobel Prize in Chemistry in 2002 [14].

The third and last feature of an ESMS setup is the fact that the species of interest is always introduced in solution. This allows for compatibility of an electrospray with many commonly used sample preparation techniques [10]. One that might come to mind immediately is the process of liquid chromatography which furthers our ability of analysis [15]. The combination of this with the other two features certainly makes the electrospray an amazing piece of instrumentation worth technical consideration.

## 1.4 Electrospray Concept of Operation

While simple in setup, the mechanics of electrospray operation are subtle and commonly disagreed upon in certain parts of the process. The general setup is a capillary tip in which a solution of electrolyte ions is present pointed towards a reduction plate seen in Fig. 1.3 below. This solution is the combination of generally a polar solvent and anything that can be dissolved in it. This rather large list includes alkali ions, alkaline earths, transition metals and their complexes, protonated organic bases and deprotonated organics acids or organophosphates.

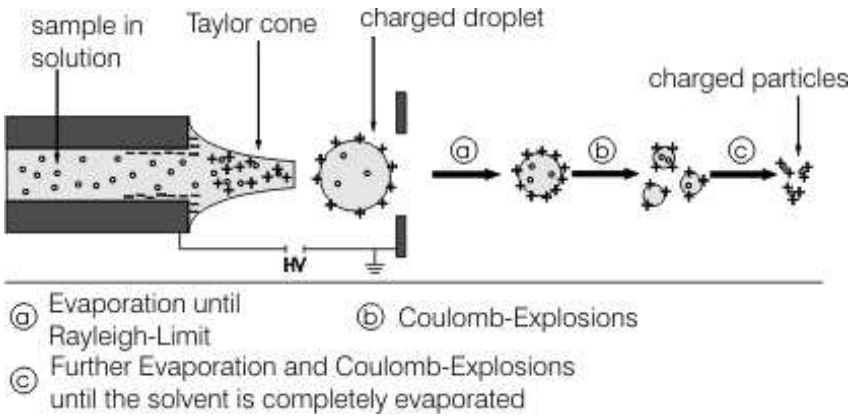


Figure 1.3: Cutout view of the electrospray setup [16]

A large potential is applied to the capillary in which this solution is fed such that the meniscus at the end is disrupted due to the repulsion of like charges leading to the formation of a liquid jet. The conditions leading to this effect as well as the properties of the droplets leaving the jet can be predicted with a combination of theoretical and semiempirical equations. As the droplets travel after leaving the cone, they undergo a solvent evaporation over time at constant charge. The decrease in radius of a droplet at this constant charge causes the droplet to approach the Rayleigh limit. At (or near) the Rayleigh limit, the particle undergoes a Coulombic fission event due to charge repulsion overcoming the surface tension force [10].

This process occurs until particles are close to the AMU mass range. Here, the resulting child particles and parent particle either goes through more evaporations (The Charged Residue Model ) or individual charged ions stochastically get ejected from the droplet (The Ion Evaporation Model). The difference between these two models is a hotly debated subject and still an open problem. The best consensus is that for certain mass of species and volume of the droplet regimes, one dominates the other but both may happen [10].

The end result of the process is generally a molecular ionized gas that is the species of interest with an integer amount of the solvent attached to it. An example of such a spectrum can be seen below in Fig. 1.4. Often this is multiply charged. When the spectrum of the solvent is subtracted off the signal, one can determine information about the species of interest.

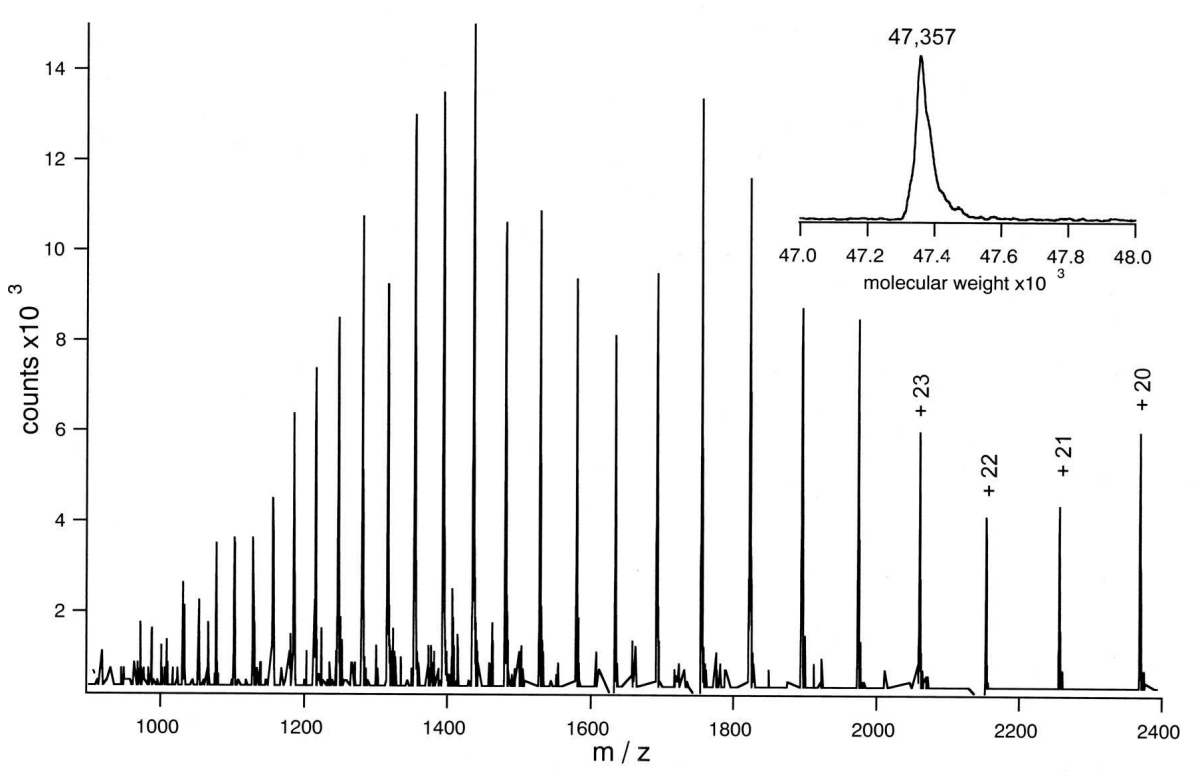


Figure 1.4: Example output spectrum of a 47kDa protein. Take note the corrected peak in the top right compared to the raw output below. What would be seen in a mass spectrometer is the species mass plus integer amount of carrier solvent [17]

# CHAPTER 2: PREVIOUS STUDIES

Previous studies computationally considering the electrospray are slim. Due to the ”shot-gun” nature of an electrospray ionization source, most literature considerations of the subject investigate the potential uses of different varieties of the system setup or probe the nature of the Coulombic fission processes as species transition into a molecularly ionized gas. However, some studies have used SIMION as a computational tool as an approach to certain problems.

Strongest among these studies is by Pauly *et al.* investigating different geometries at the vacuum interface of an arbitrary atmospheric pressure ionization system [18]. This study utilized SIMION in order to predict ion currents of select species flying through these geometries with constant mass. Their results were overwhelmingly positive, with a configuration that increased yield from 10% of particles to 100%. While these results are certainly meaningful, the approximation of constant mass is a difficult assumption to make when translating the geometry to a real-world experimental setup.

Previous experimental analysis of certain setups have concluded that ion current yield is very sensitive to time-of-flight as the enabler for extended charged droplet desolvation and a greater number of fission events [19]. This calls for a more careful consideration of how one treats flying particles in ESMS systems. Even more concerning is further experimental evidence that there is a strong spatial sensitivity of the position of a spray source [20]. The combination of these two results proves that in order to find that ”sweet spot” of ion current, it’s necessary to develop a model that carefully considers spatial aspects of the system and accurately includes consideration of evaporation/fission processes. Fortunately, procedures such as these analyses have contributed to the development of experimental high-yield system setups before [21].

In order to correctly define the initial particle, previously determined theoretical expressions for initial radius and charge must be used. These expressions have been shown to correctly represent experiment over several different solvents and contexts. The initial radius R, and charge q of an example particle leaving a standard, one mode, Taylor cone goes as follows [22].

$$R = \left( \frac{3\epsilon\gamma^{1/2}V_f}{4\pi\epsilon_0^{1/2}KE_c} \right)^{2/7} \tag{2.1}$$

$$q = \frac{1}{2}8(\epsilon_0\gamma R^3)^{1/2} \tag{2.2}$$

where,

$R =$ radius of the droplet produced

$q =$ charge of the droplet produced

$\gamma =$ surface tension of the solvent

$\epsilon =$ permittivity of the solvent

$\epsilon_0 =$ permittivity of vacuum

$K =$ electrical conductivity of the solution

$V_f =$ flow rate of solution

$E_c =$ applied electric field at capillary tip

where this $E_c$ is approximately by the expression below [22, 23]

$$E_c = \frac{2V_c}{r_c ln(4d/r_c)} \tag{2.3}$$

where,

$$V_c = \text{applied voltage to capillary tip}$$

$$r_c = \text{capillary outer radius}$$

$$d = \text{distance to the first counterelectrode}$$

After the initial setup, the particle, or droplet will fly down the lensing geometry, undergoing many Coulombic fission events before finally making a final transition into molecularly ionized gas. These Coulombic fission events occur at the Rayleigh stability limit shown below in terms of previously defined variables [24].

$$q_{Ry} = 8\pi(\epsilon_0 \gamma R^3)^{1/2} \tag{2.4}$$

This stability limit can be interpreted similarly to how a droplet leaves the end of the capillary. For a certain radius of the droplet, a charge $q_{Ry}$ is needed before mutual repulsion breaks apart the droplet.

## 2.1 Thermal Evaporation

How a droplet reaches the Rayleigh stability limit is through solvent evaporation. This solvent evaporation takes careful consideration however as the electrospray operates in a different regime than conventional hydrodynamics.

### 2.1.1 A first attempt using Fick's Laws of Diffusion

Fick's Laws of Diffusion is a well known, well studied, law that predict a steady state diffusion coefficient for a surface. This diffusion constant can be interpreted as a mass flux of phase transition and bears a remarkable similarity to flux in Maxwell's equations that physicists will be more accustomed to. Fick's Laws have several assumptions built into them when considering phase transitions that will be found to be broken in this special case and subsequently will

mandate a different approach.

Safely assuming the droplet is spherical, the expression for mass transfer $\dot{m}$ as a function of droplet radius $R$, diffusion coefficient $\nabla$, and the change of vapor concentration with respect to radius $\left(\frac{dc}{dr}\right)_{r_a}$ can be written as thus.

$$\dot{m} = 4\pi R^2 \nabla \left(\frac{dc}{dr}\right)_{r_a} \tag{2.5}$$

Fick's law also gives an expression to establish the proportion of flux to concentration gradient.

$$\frac{\partial c}{\partial t} = \nabla \left(\frac{2}{r}\frac{\partial c}{\partial r} + \frac{\partial^2 c}{\partial r^2}\right) \tag{2.6}$$

Near the surface of the droplet building off of the steady state assumption of the surrounding environment, the following expression can be set $\frac{\partial c}{\partial t} = 0$ which leads to new expression.

$$0 = \nabla \frac{2}{r}\frac{\partial c}{\partial r} + \nabla \frac{\partial^2 c}{\partial r^2} \tag{2.7}$$

This is a differential equation solved by the following solution.

$$\frac{\partial c}{\partial r} = \frac{A}{r^2} \tag{2.8}$$

Where $A$ is a constant with all the absorbed factors within it. Plugging into Equation 2.5 and solving for $\left(\frac{dc}{dr}\right)_R$ leads to.

$$\frac{dc}{dr} = \frac{\dot{m}}{4\pi \nabla r^2} \tag{2.9}$$

Integrating this expression over the bounds of the system in $r$ results in

$$c_{r_a} - c_\infty = -\frac{\dot{m}}{4\pi\nabla r_a} \tag{2.10}$$

The ideal gas law, applicable under this situation will lead to an expression of the concentration as a function of molarity $M$, gas constant $R_g$, pressure $p$ and temperature $T$.

$$c_x = \frac{Mp_x}{R_g T_x} \tag{2.11}$$

Implementing this will lead to our final expression

$$\frac{\dot{m}}{4\pi r_a^2} = -\frac{M\nabla}{r_a R_g}\left(\frac{p_a}{T_a} - \frac{p_\infty}{T_\infty}\right) \tag{2.12}$$

Where the left side of the equation can be interpreted as the diffusion per square area on the sphere. There are many things to mention about this expression yet as it turns out, it doesn't work for the electropray. This expression, which now represents the mass flux of a sphere falls apart for two reasons. First note the trend of the flux as radius, $r_a$ approaches zero. As this happens, the predicted flux increases dramatically and results in misrepresenting flux in the case of small droplets where other dynamics must be considered.

Secondly, this approximation also fails in the case of large differences on the concentration gradient on the boundary. While the difference between a droplet and atmospheric pressure is acceptable, the difference between droplet and any reasonable vacuum (as seen in all electrospray systems eventually) is not so much so.

### 2.1.2 A second attempt using gas kinematics

With this all in mind, a different consideration of the system is needed that will leave something different yet with noticeable features that are flexible in what limited our previous expres-

sion. Borrowing from kinetic theory, an expression for the total particles that interact with a boundary at any time in the opposite direction of diffusion (inwards in this evaporation phase) can be written as such.

$$\frac{1}{4} n c_{sat} \bar{v} * 4\pi r_a^2 \text{molecules/second} \tag{2.13}$$

Where $c_{sat}$ is the concentration at saturation, $\bar{v}$ is the mean of the velocity of vapor particles, n is the saturation vapor concentration, and $r_a$ is again the radius of the droplet. Unfortunately, this is where theory ends and empirical methods must be used as what happens on the molecule by molecule basis during the phase transition is unknown. Now introduce condensation coefficient $\alpha$ which represents the proportion of particles that adhere to the surface against those that redisperse. When the vapor-liquid boundary is saturated in isothermal conditions, the exchange of particles is equal and the condensation coefficient is equal to the evaporation coefficient which is interesting in determining thermal evaporation.

In all cases up to the current date, the evaporation coefficient is determined by careful experimentation. When the ideal gas law is used to solve for densities similar to above, the expression that correctly expresses the maximum mass rate of change for the solvent of interest can be written.

$$\frac{\dot{m}}{4\pi r_a^2} = -\frac{\alpha \bar{v}}{4} * \frac{M}{R_g} \left( \frac{p_a}{T_a} - \frac{p_\infty}{T_\infty} \right) \tag{2.14}$$

In this formula, as opposed for the one above, the diffusion of the solvent has been replaced with a particle by particle consideration $\alpha$ at the cost of empirical determination. Fortunately, the particulate in ESI used in this simulation is along the lines of known evaporation constants which leads to a new well-defined surface evaporation limit law. This establishes the radius as a function of time and known parameters [25].

$$R = R_0 - \frac{\alpha \bar{v} p^\circ M}{4 \rho R_g T} t \tag{2.15}$$

where,

$\bar{v}$ = the average thermal velocity of solvent vapor

$p^\circ$ = the saturation vapor pressure of the solvent at the temperature of the droplet

$M$ = molar mass of solvent

$\rho$ = density of solvent

$R_g$ = gas constant

$T$ = temperature of droplet

$\alpha$ = condensation coefficient of solvent

It should be noted that these parameters are mostly determined in vacuum and many, especially the condensation coefficient, may change drastically in differing pressures of the system. Many applications of the electrospray start at pressure higher than vacuum and many more at atmosphere. It is not known the exact nature of how the theory of gas kinematics might affect the evaporation of the solvent although it is safe to assume that it will only hinder it.

## 2.2 Child Particles

While the processes leading up into the Coulombic fission events are well known, the nature of resulting child particles is much less so and consequently the largest source for ambiguity in this project. Authors have explored this topic with only approximate results. It is known that the process is ”uneven fission” or ”droplet-jet fission” [26]. This was explored by Gomez and Tang [27] with methanol to produce an average of twenty particles totaling 2% of the parent mass and 15% of parent charge which are the numbers used in this paper. Other sources have shown that the ranges of percent charge and percent mass loss associated with the fission process can vary by a few percentage points around those numbers [28]. Below in Fig. 2.1 is a diagram

detailing an observed breakup of a methanol-based spray.

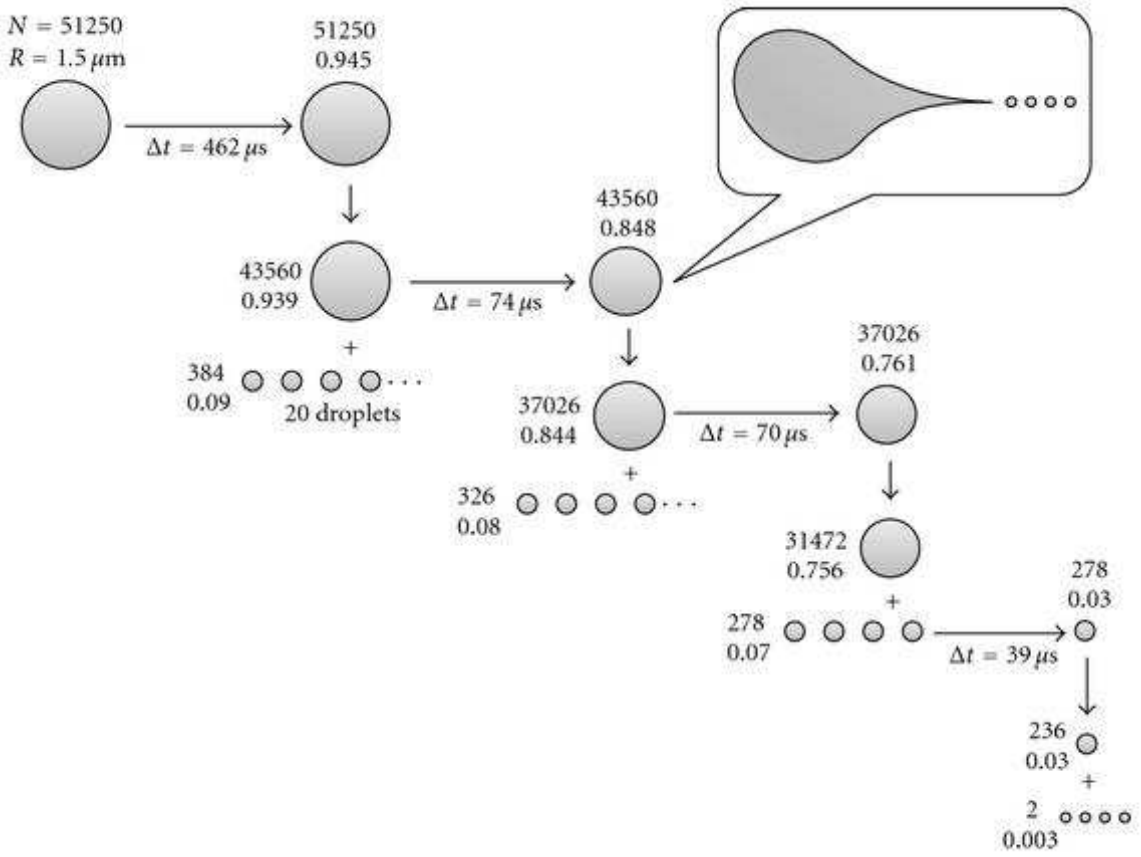


Figure 2.1: A state diagram of an observed breakup of a methanol droplet through four generations. N refers to number of elementary charge and R to the radius in micrometers. In the top right is a sketch of how the process looks [26].

More recent papers have given quantitative expressions detailing the breakup for polar solvent more clearly. For example, Fernandez de la Mora has proposed, along with some more qualitative statements, that the diameter of an offspring particle corresponds to the expression below [29].

$$d_m \approx \left(\frac{\gamma}{\rho}\frac{\epsilon}{K}^2\right)^{1/3} \tag{2.16}$$

With new constants $K$ as electrical conductivity and $\rho$ as density. Due to the uncertain nature of this expression as well as the lack of a quantitative description of the resulting charge of the child particles, this expression was excluded in favor of the methanol data found by Gomez and

Tang.

The transition of the droplet from a ”macroscopic” droplet to a molecular ionized gas is contested in literature between two different theories. The first, proposed by those who first developed the ESMS system, postulates that solvent evaporation continues down to the point of a gas phase ion [30]. This *charged residue method* has shown to have some support in later literature although its rival has been investigated much more.

The other mechanism is, as opposed to solvent evaporation, *ion evaporation*. In this model, proposed by Iribarne and Thomson [31, 32], the droplet's inhomogeneity allows for the chance for a single ion to escape the droplet when it reaches a certain size and becomes the dominant mechanism of mass change when radius decreases past ten nanometers. There appears to be a wealth of literature supporting this theory although nothing that can successfully conclude that the ion evaporation or the charged residue model accurately predicts the behavior of the transition. One mechanism may seem more dominate than the other on a case per case basis. For simplicity, the charged residue model has been assumed for the purpose of this simulation.

# CHAPTER 3: APPROACH AND METHODS

Detailed below is a description of the methods in which the theory of the electrospray was represented in simulation.

## 3.1 SIMION

The simulation of the process leading towards the creation of an electrically charged aerosol was carried out in SIMION. SIMION is a finite element solver for ion optics. It supports user defined electrode geometry and solves for the potential map of a user defined region. Particles may then be defined and "flown" in this space. It is thus ideal for exploration projects dealing with mass spectrometry, its most common use. SIMION does not fully support particle interactions but it supports the scripting language Lua which may be used at certain junctions of a finite element solving process. It is with this that the creation of the aerosol is implemented.

### 3.1.1 Geometry

At the beginning of the process leading into a simulation, the user defines a rectangular grid space in which their system exists. This region will be later integrated over to develop the potentials which encourages minimization to be prioritized to preserve computational time. Units may then be assigned to the space. In this instance, grid distances are set to the millimeter. An immediate and legitimate concern in determining electrically potentials is the edge effects associated with approaching sharp corners. SIMION assumes that dynamics of interest will happen at sufficient distance from sharp points and assures that flat edge effects are correct. This flat edge assumption has to be accurate or else it will drastically affect the acceleration a droplet will experience from the highly charged electrospray needle as the needle can only be as small as the grid size. Since a dominating majority of the particles acceleration is in the axis of the direction of the needle, it is assumed that the edge effects can be forgiven as the particles creation will be a flat edge between the sharp points.

Another methodology to deal with the sharp point problem might be to simply define the grid size on the order of magnitude of the dimensions of the needle. This is the nanometer regime. Unfortunately, SIMION requires 10 bytes of RAM per grid point. This puts modeling

a nanoscale-defined potential at the centimeter level needing a minimum of 10 zettabytes of RAM. This shoots down this approach although small gains in resolution might still be possible.

### 3.1.2 Finite Elements

After the electrode geometry is defined, SIMION numerically integrates over the space to determine the potentials at each grid unit. With electrodes in consideration, geometries are then used to solve Laplace's equation show below [33].

$$\begin{aligned} \nabla^2 V &= \nabla \cdot \nabla V = 0 \\ \nabla V &= \frac{\partial V}{\partial x} i + \frac{\partial V}{\partial y} jl + \frac{\partial V}{\partial z} k = E \\ \nabla^2 V &= \nabla \cdot E = \frac{\partial E_x}{\partial x} + \frac{\partial E_y}{\partial y} + \frac{\partial E_z}{\partial z} = 0 \end{aligned} \tag{3.1}$$

SIMION uses a finite difference over-relaxation technique with Eq 3.1 in order to integrate and find voltages at each grid point in the space. These voltages are then used to determine the the continually changing position, velocity, and acceleration of particles as they fly per spatial step defined by the user up to a maximum spatial resolution of $1/500th$ of the minimum grid size [33].

One option present in SIMION that is utilized in this simulation is skipped point refining. As stated above, SIMION uses a relaxation method in determining its potential field with a convergence aim. Relaxation methods tend to scale as $n^2$ thus making refining significantly slower and often out of the scope of the time where a simulation is still interesting. Skipped point refining divides the space by factors of two until the array is small enough that the convergence goal can be reasonably reached in time. The space is then redefined with one less factor of two resolution with the potentials set to the solutions just found. This process continues until the convergence goal is met at the maximum resolution or rather, the originally defined grid size. This method significantly decreases refining time and works well with linear gradient schemes which is the case in electric potentials. Another added benefit is the ability to overcome the preferential treatment of the regions surrounding a source in relaxation methods. The only disadvantage present in this method is the ability to miss smaller electrode geometries in a

system due to being averaged out. This is compensated in SIMION by flagging spaces where it knows electrodes are present and averaging around that [33].

### 3.1.3 Lua Integration

As mentioned above in section 3.1, SIMION allows for integration with the scripting language Lua. Lua is generally used in graphics programming and seems almost an odd choice for scientific computing but it ends up being a powerful tool in the context of SIMION. It allows for the writing of reserved values, values that SIMION calls during runs, in the software. These could be the properties of the particle as well as the electrodes and any calculation one could implement with the code.

These features are how the complexities of the aerosol formation are implemented. The code is compiled at the beginning of the simulation run and recognized globally. Functions that are pre-coded to be searched for in SIMION can then be written to influence the simulation at certain steps. Examples include initialization of a run, each time step, and post-processing at the end of a run. As such, there are multiple ways to implement theories that are not already included in the program.

SIMION assumes particle conservation. Consequentially, the transition of the consideration of one droplet into many particles is something that needs to be ”forced” by Lua code. This was achieved by creating a list at the beginning of the code which is called at each time step to determine the properties of the particle being run. When a droplet undergoes coulombic fission, particles are created and the list is appended with the determined initial conditions of the new particles.

Also, at each time step is the calculation of the loss in mass due to thermal evaporation as well as the calculation of the Rayleigh limit that corresponds to the radius of the charged particle determined by its mass. A catch in the code is implemented to ensure that the mass does not become lower than the limit of ion evaporation, the mass of the solvent. In essence, particles evaporate only if they are above their fundamental lower limit. This ends up being a robust method that appears to correctly represent the underlying physics presented in the code. A copy of the exact code used in the simulation can be seen in Appendix A.

### 3.1.4 Weaknesses

Lua itself becomes limited in its nature due to its lack of support outside of documentation that comes as examples with the installation of SIMION itself. It was sufficient however in completing the desired goal although the possibility of a simpler syntax or methodology of implementation still exists and might have been possible under a more supported code base.

The actual simulation SIMION side is robust and believed to be accurate within the extent of its use within this context. The biggest source of ambiguity with SIMION is the accuracy of edge effect which is assumed to be accurate by claim of the developers of the software [33].

## 3.2 Geometries of Interest from Outside Sources

This section highlights some example systems from instrumental optimization papers as well as patents on the subject of ESI sources. They all will serve as example geometries and inspirations for the geometries that end up being simulated. There is an obvious complexity in some of these examples that will not be represented in simulations as they are outside the scope of this project. However these geometries indicate that the simulations presented in this document are on the right track.

In this first lensing proof of concept below in Fig. 3.1, the authors consider a nanospray source aiming for a orifice. They highlight the trajectories of ionized particles as well as equipotential lines. The voltages used in these simulations are on similar magnitudes of the voltages used in this paper. The authors concluded that yield was increased which could be easily duplicated [34].

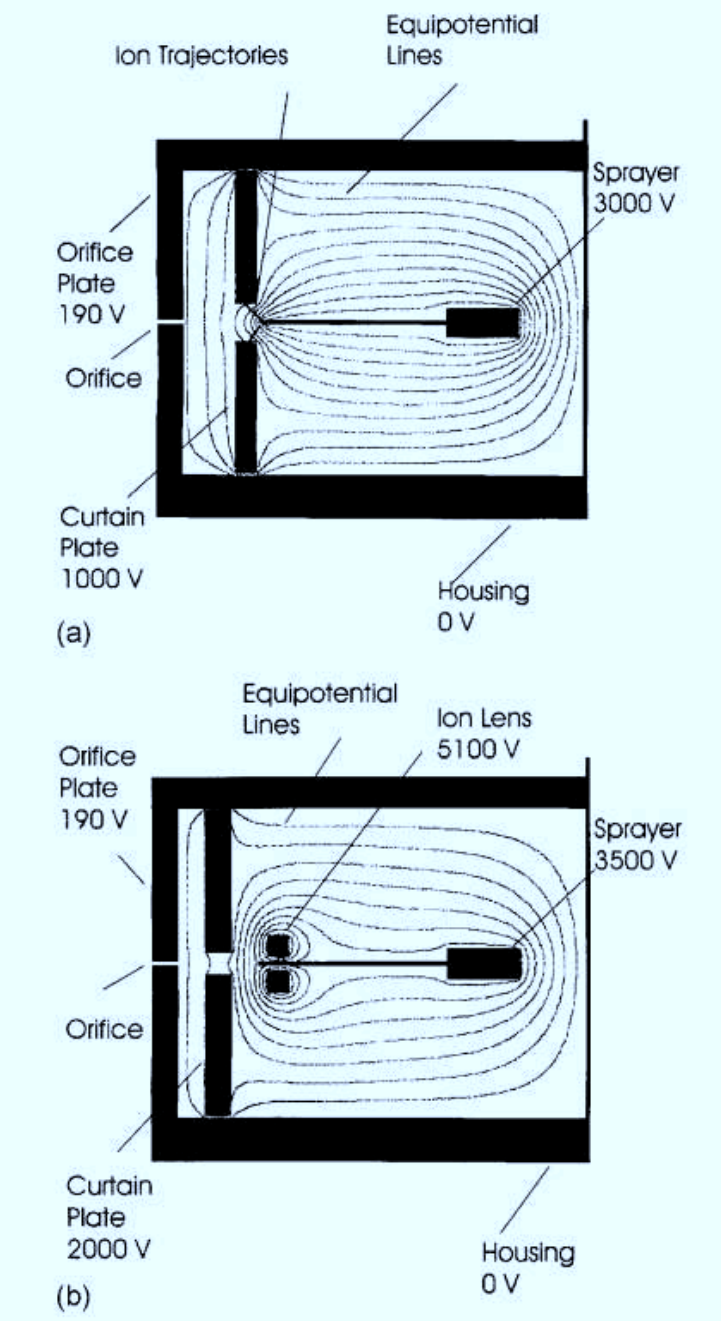


Figure 3.1: Ion trajectory optimization from sprayer example [34]

In a later paper by the authors of Fig. 3.1, an off-center spray source situation is presented in Fig. 3.2 allowing for the elimination of neutrals while still allowing for ion transmission. Identical information is presented showing the potential use of lensing in cases where trajectories may be at an off angle. Again, this can easily be replicated [35].

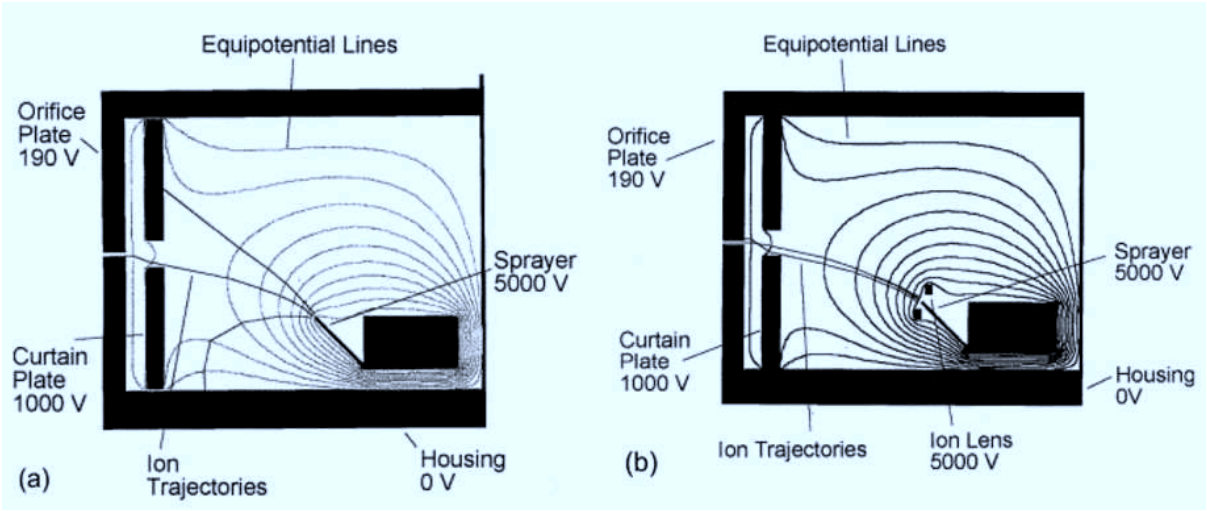


Figure 3.2: Off axis ion trajectory optimization from sprayer example [35]

When looking at patents as in the below Fig. 3.3 that contain a little more detail, one can see the added complexities that are introduced into actual systems. Drying gases are included along with a heated capillary and multiple charged plates and skimmers are within a differential pumped vacuum system [36].

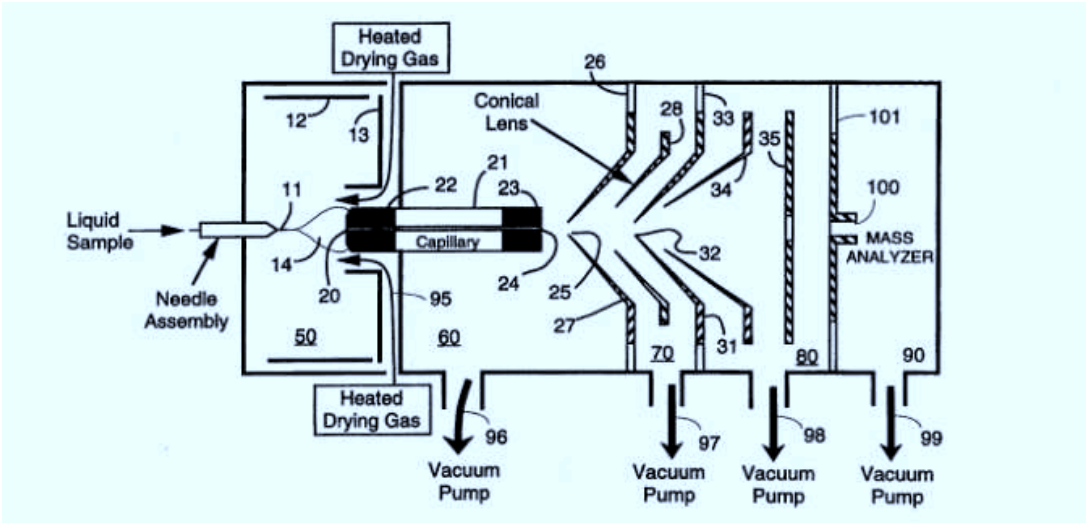


Figure 3.3: Ion lensing electrospray complexity example [36]

Fig. 3.4 is another similar patent with one new feature of the nozzle for the ESI system being pointed downwards ninety degrees off-axis. This causes the majority of neutrals produced from the spray to miss the inlet and only charged particles to be drawn in. This setup is actually relatively common, or rather, the concept of an off-center aimed nozzle is. This is an important characteristic of many systems and might be a point of investigation [37].

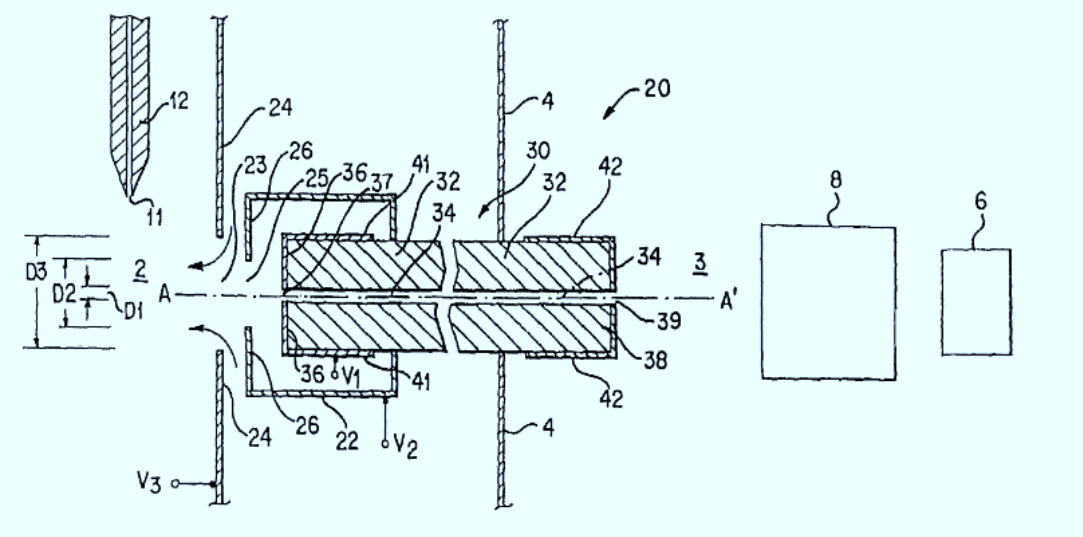


Figure 3.4: Perpendicular spray electrospray setup [37]

Another method of eliminating neutrals could be physically blocking them down the travel path as ions get guided around. This idea is borrowed from inductively-coupled-plasma mass spectrometery where photons are created by the plasma at the start of the ionization process and need to be blocked or else they incur an interference with measurement instrumentation [38]. Seen in Fig. 3.5 this ”shadow block” is a concept the USGS is exploring for its electrospray lensing setup and thus represented in the third simulation presented in this thesis.

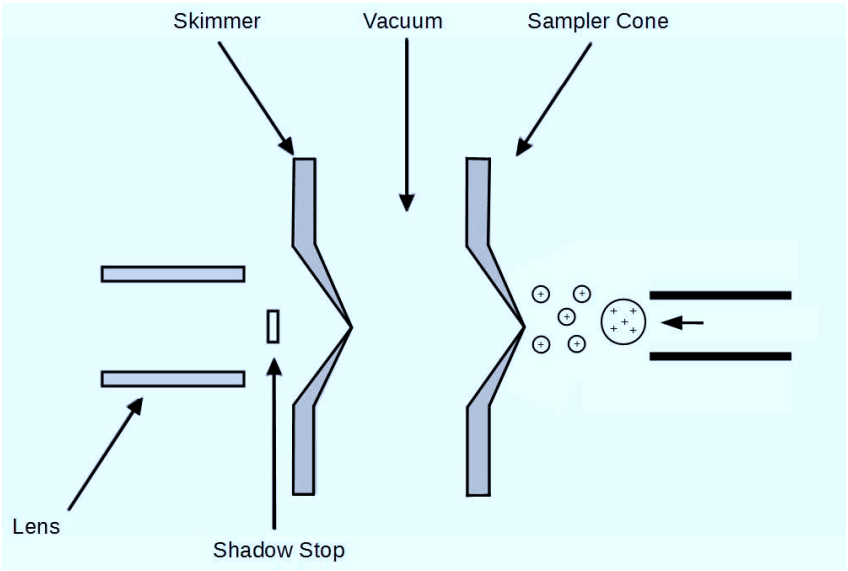


Figure 3.5: Example layout of an ICP mass spectrometer adjusted for the electrospray

## 3.3 Assumptions and Discussion

It should first be noted that the resulting simulations from these methods will not be representative of an actual experimental setup. Presented however, is the current theory and empirical knowledge that allows for an exploratory look into simulating the electrospray. A more comprehensive understanding of fluid dynamics and hydroelectro dynamics will be needed before simulations will approach values seen in true experimental setups. That said, a careful description should be presented of the shortfalls, assumptions, and approximations seen in this simulation such that when literature is presented that correctly describes them comes to light, these problems can be relaxed.

Initial conditions of the droplet in the scope of its mass and charge are comfortably supported in both theory and practice as has been discussed. Should concentrations of the species of interest be too high to contribute a significant portion of the mass compared to the solvent, more descriptive theories should be developed. However, most applications of the electrospray as well as the goal of increasing detection limit won't be close to flirting with this limitation.

Once the particle is free of the needle, approximations become dominate in determining the dynamics of the system. As discussed in Section 2.1.2, the fact that most characteristics of the solvent are determined in vacuum hinders the ability to determine how a solvent will evaporate in atmospheric like pressure often seen in electrosprays. This can be easily rectified by measuring the condensation coefficient at differing pressures. Such experiments are difficult however and thus studies are focused more towards fundamentally describing the process of evaporation on a nano-scale although they are currently unsuccessful. It is then assumed that this model is under vacuum or a pressure whose average path length is on the order of the size of the system.

The Rayleigh limit, the theoretical upper limit of charge of a droplet before it undergoes a fission event, is not observed experimentally to be the value at which particles begins fission [27]. Values between 70% and 80% the Rayleigh limit have been seen to occur in droplets undergoing fission. Current theories speculate that there is a first mode circle oscillation that is what causes this early breakup although more investigation is needed before that can be determined conclusively [27]. Regardless, simulations presented in this thesis assume the particle's

fission events occur at the 70% mark. This is due to the observation that evaporation rates are sometimes on the same order of magnitude per time step of the mass of droplets. There will be some guaranteed overshoot past the limit on the time step determined where a fission event will occur thus the lower limit of 70% was a logical choice.

These things in mind, the largest source of ambiguity in the system is the characterization of the child particles. Knowledge of these particles is best characterized experimentally in methanol and thus methanol was chosen as the solvent of choice for these systems. Literature is limited to describing the fission products as percentages of the initial mass and charge as well as an approximate number of offsprings. This is empirical and possible parameters in the system or of the solvent that might change the number of fission products (twenty in this case) are not known. This limits the scope of the analysis to methanol and caution would have to be observed to stray from it.

Twenty particles implies that in the case that parent particles aren't considered, the total amount of particles scales as $20^n$ where $n$ is the number of fission events that occur before the droplet runs against the mass lower limit or the limit of $1e$ charge. This is only if the simulation is restricted to ignoring the resulting parent particles of any one fission event. Keeping parent particles incurs another $20^{n-1}$ particles itself. This fact results in simulations that always result in a number of particles equal to the total amount of elementary charge units present in the initial droplet which in itself isn't realistic. The resulting approximation that is made in simulations presented here is that any parent particles are not considered. This prevents longer computational time but also means that mass is not conserved in the system. This in mind, a velocity correction factor for the loss of kinetic energy is something that in future simulations should be considered.

Outside of theory, it is assumed that SIMION correctly represents the physics that it is told to describe. Potential problems with edge effects and their resolutions are discussed in Section 3.1.1.

### 3.3.1 Beam Divergence

The charged particles within this simulation move under the effects of the electrodes but they themselves produce a potential that at certain densities and distances that may contribute to their individual movement. This effect results in a beam divergence that should be considered in this simulation for it would introduce a divergence correction or deemed unnecessary.

In order to characterize this effect an analogous, well known, method for determining the angular divergence of an electron beam is used. Consider a test particle at radius $r$ from the center of the beam path. Rewriting the integral form of Gauss' law for a cylinder centered on the beam's directional axis, the expression for electric field is below in Equation 3.2.

$$E_r(r) = \frac{1}{\epsilon_0 r} \int_0^r \rho(r) dr \tag{3.2}$$

Integrating with respect to $r$ leads to an expression for electric field felt by a particle within the beam.

$$E_r(r) = \frac{\rho r}{2\epsilon_0} \tag{3.3}$$

The force felt by this particle will obey the Lorentz force law seen below in Equation 3.4.

$$\boldsymbol{F} = q(\boldsymbol{E} + \boldsymbol{v} \text{x} \boldsymbol{B}) \tag{3.4}$$

The magnetic field component of the above equation is resulting from the "current" of the moving charges. In a non-relativistic setting, this component is effectively zero. With a charge density resulting from Equations 2.1 and 2.2 of $5.8$ x $10^{11} C/m^3$ and the mass of a test methanol particle of 32 AMU, it can be determined that the acceleration of one such particle at the edge of a droplet would experience a divergence of $1.5 cm/s^2$ away from the beam axis. Using accelerations taken from simulations found in Chapter 4 of a droplet around the needle point,

the resulting angular divergence of $3$ x $10^{-9} radians/sec^2$ is found. Acceleration of the droplet in the axis of it's motion is so great close to the needle where it's charge density is highest that any transverse spread can be ignored. It is thus deemed that beam divergence is not a contributing factor to this study.

# CHAPTER 4: RESULTS AND DISCUSSION

Three geometries were explored with the simulation of the electrospray process. One being the free space case to highlight the dynamics of the system, another being the off axis input, and finally one with a drying plate often seen in ICP-MS. As mentioned previously, the solvent used was methanol to match values used in previous literature. Using the same values found in Tang and Kebarle, the initial radius and charge of the particle was determined to be $1.5\mu m$ and $8.2$ x $10^{-15}C$ respectively. The thermal evaporative radius loss was similarly determined to be $1.2$ x $10^{-3}m/s$ [39]. Corresponding stability limits for a particle as they fly was determined by Equation 2.4 and the limit of 70%.

A small arbitrary off axis spread was included as an addition to velocity as part of the simulation at each fission event. This is both to describe the uneven nature of the fission but mainly to highlight dynamics of the system that would normally overlap and not be visible. This spread is determined randomly about the direction of motion for the particle which is approximately even for the twenty offspring particles.

The size of the system in each simulation is $10cm$ X $10cm$ X $40cm$. These numbers are larger than actual experimental setups in which most are on the order of a few centimeters. Once it was found that the first fission event happens at around that distance in many cases, it was decided that geometries should scale up rather than manipulate the properties of the droplet for faster fission so these properties could continue to match those found in literature. This limitation must be maintained as the fission process could have unknown dependencies on solvent droplet properties such that a droplet that has an earlier fist fission event might have drastically different fission results.

## 4.1 Free Space Needle

The first case deals with the needle in free space of the size of other systems. Below in Fig. 4.1 is pictured the resulting trajectories of the particles in this case.

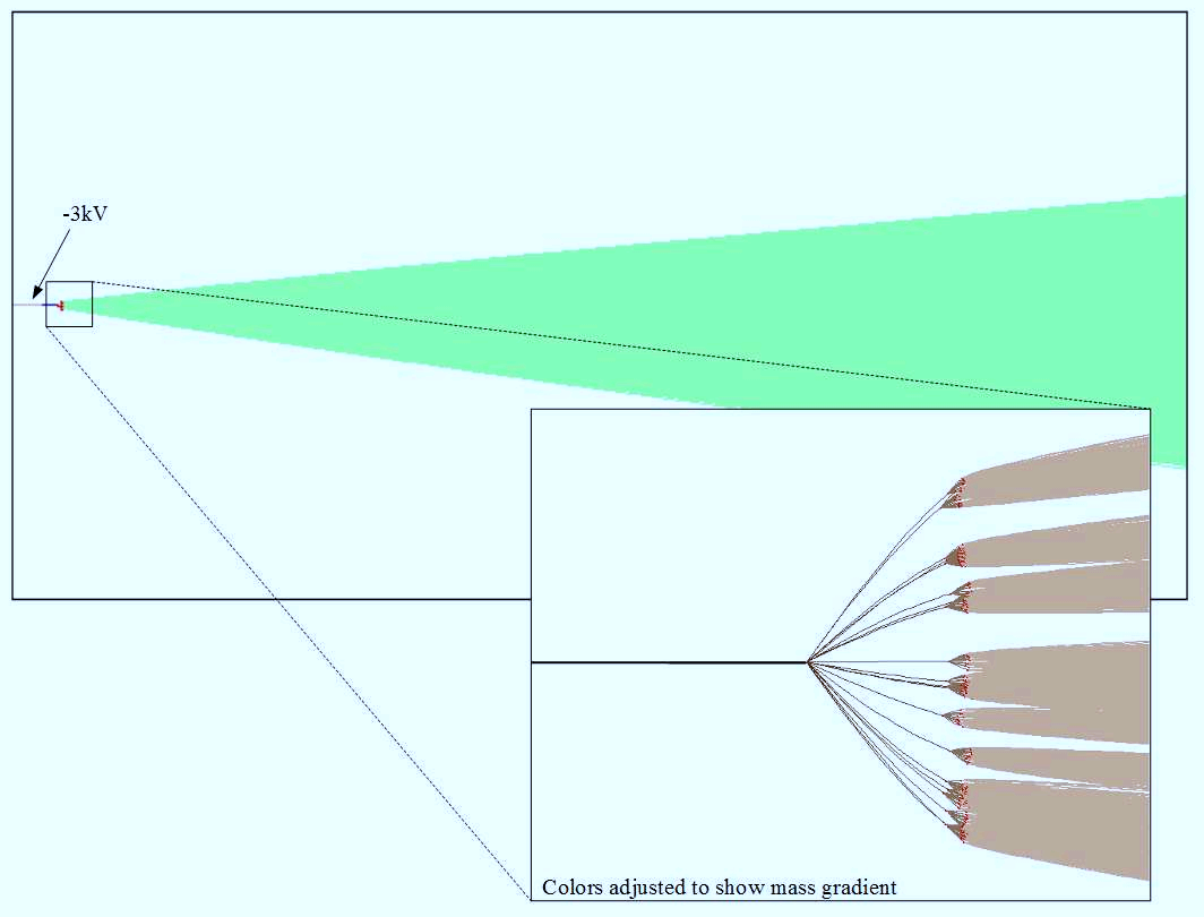


Figure 4.1: A lens free simulation of the electrospray process

The arbitrary spread of the particles is particularly noticeable here as the paths aren't manipulated by any sort of lensing geometry but this will be seen to dissipate somewhat later. The time to first fission event is about $700\mu s$ with total particle travel time varying between $1000\mu s$ to $1100\mu s$.

The zoomed in cutout shows the plume process. It's notable here that the transition from initial droplet to aerosol happens with an exponential faster rate to successive fission events due to a constant rate of evaporation. Because of this, regardless of particle size, the plume is extremely small on the scale of time and distance of the process. This implies that perhaps it is more important to use analysis to determine the point of the first Coulombic fission event rather than the lensing of a changing mass. This theme is one the will be seen repeated in the next two geometries. An isometric view of the spray in free space is below in Fig. 4.2.

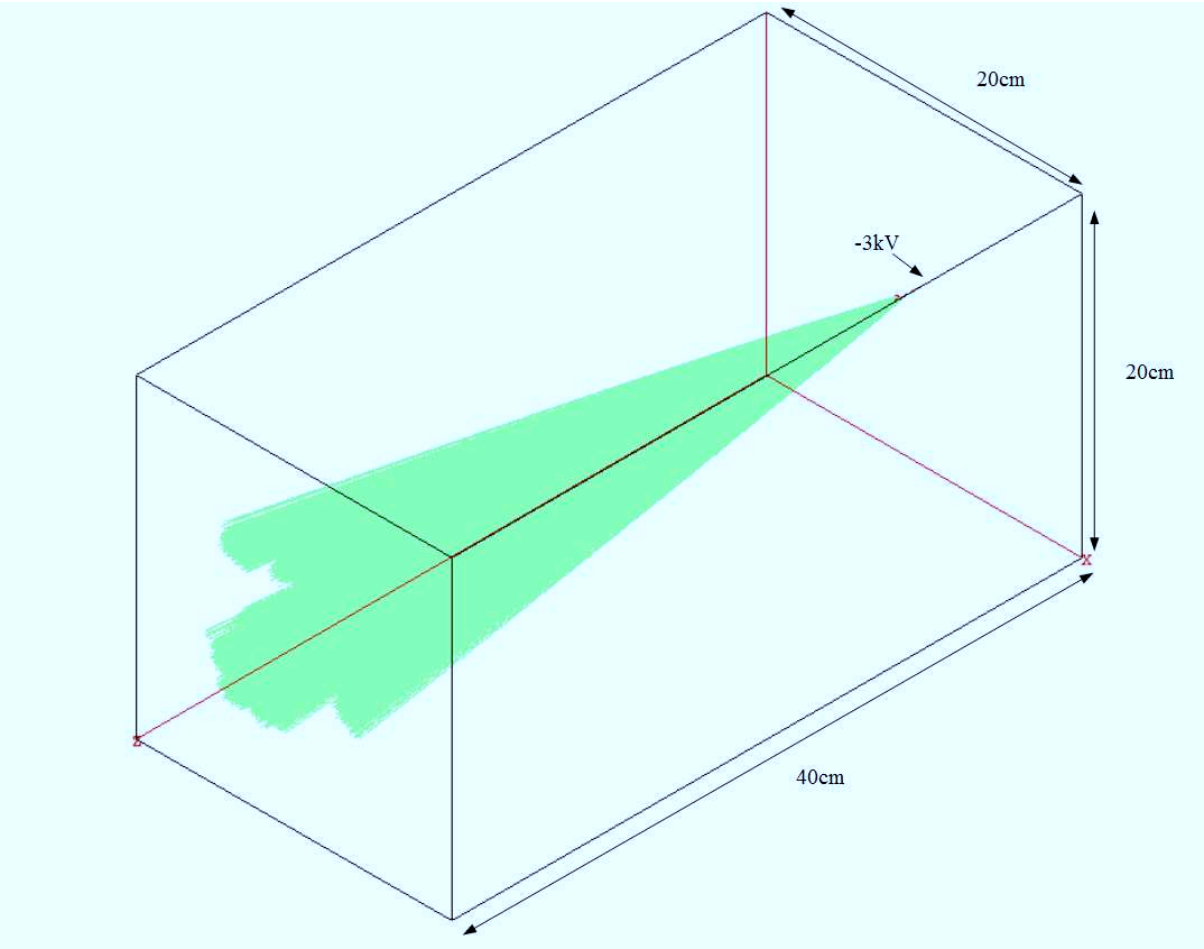


Figure 4.2: An isometric view of the free space needle spray.

## 4.2 Off-axis orifice with deflector plate

In the first of the two geometries with focusing electrodes, the off-axis input is considered. This is represented in this first order approximation of a similar experimental setup comprised of a circular plate with an orifice and a flat deflector plate across and slightly shifted from it. This geometry is highly inspired by the off-axis input geometry presented in Section 3.2. A view of the setup can be see below in Fig 4.3.

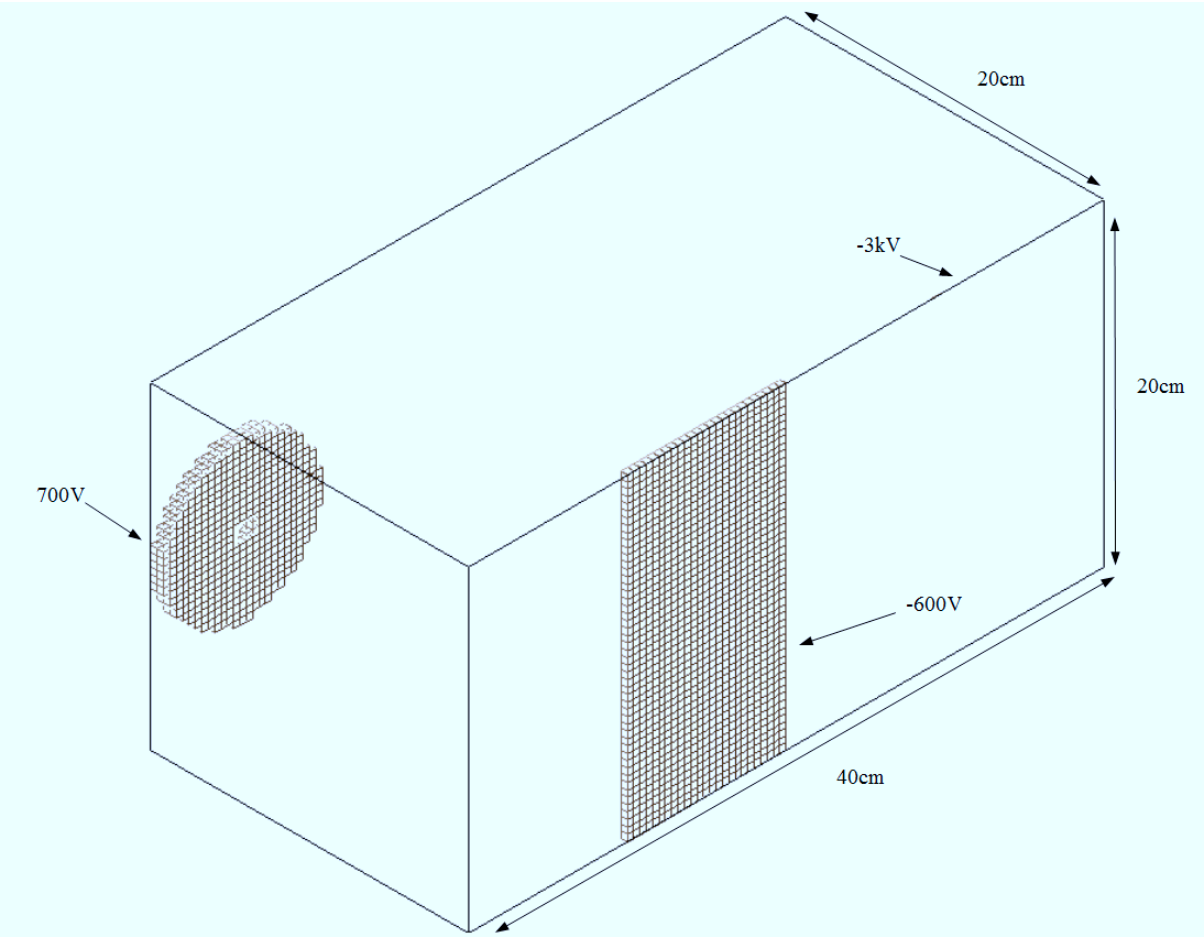


Figure 4.3: A view of the setup for the off-axis case with deflector plate.

Voltages were set manually, leaving the option for potential configurations that might increase yield. The contour map the the above setup is presented below in Fig 4.4.

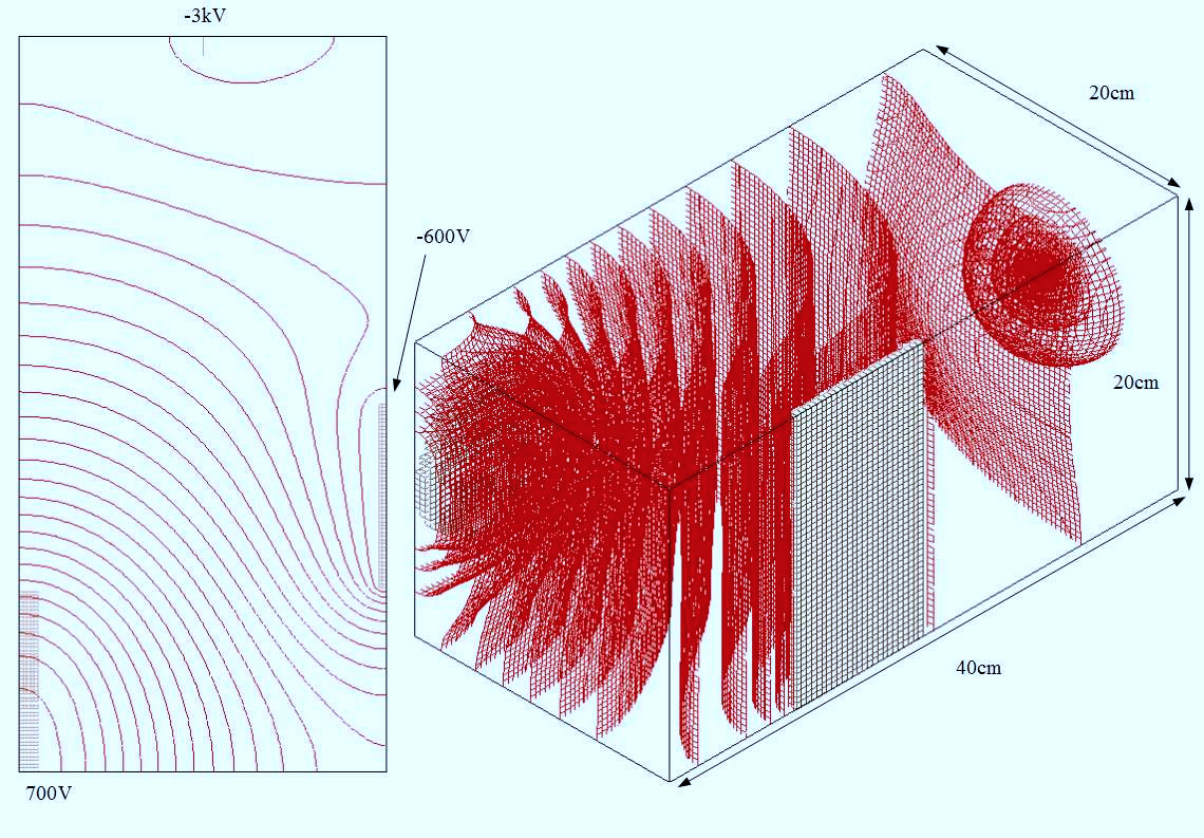


Figure 4.4: A potential contour plot for the off-axis spray with deflector plate geometry

Contour resolution was selectively chosen so that the changes in the potential are best visible. It can be seen that a simple geometry conceptually can result in a potential that would have been theoretically challenging justifying the need for numerical consideration. The droplet and resulting child particles will follow these lines and result in the trajectory plot shown below in Fig 4.5

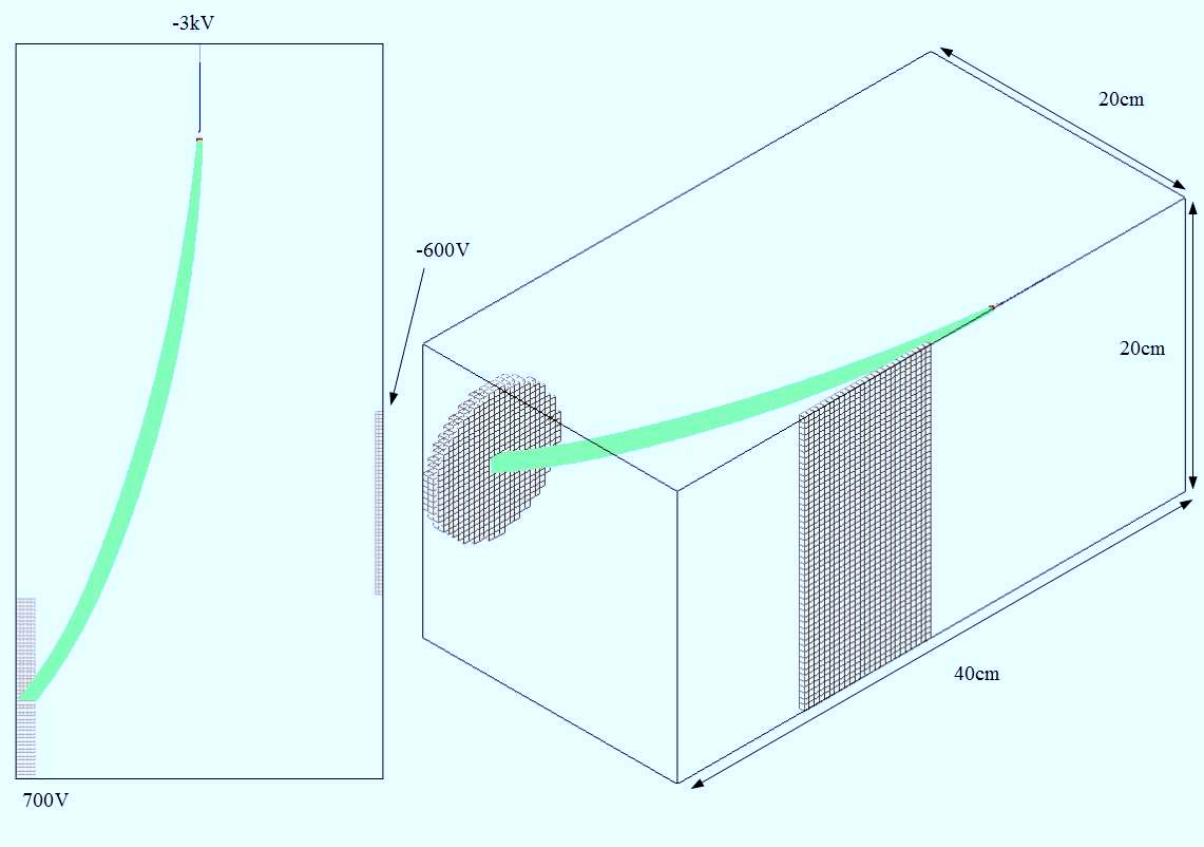


Figure 4.5: Spray simulation for the off-axis spray with deflector plate

It can be seen that the geometry is successful in guiding the particles into the orifice. Without the spread it is, in fact, a 100% yield although a sharper entry angle might be more desirable in a system which would continue down the line of the orifice. This 100% yield isn't the total charge of the initial droplet but the charge of the first generation offspring particles without the parent particles as was discussed in Section 3.3. This yield is the product of three fission events which can be observed in the previous geometry. As each fission event keeps 15% of the parent particle's mass, it can be determined that a 100% yield of simulated particles corresponds to a 0.034% yield of initial droplet charge.

As the first lensing geometry, this system can be used to give a little insight as to what would happen should parent particles be included in the simulation. Below in Fig. 4.6 is the resulting trajectories of the particles. Since the original reason the parent particles were excluded was to save computation time by eliminating total particle count, the number of offspring particles for each Coulombic fission event was set to one to preserve that simplification somewhat. The child particle still retains the mass and charge as if it was one of the twenty that would be present in a

full simulation. The artificially spread is also excluded to see exclusively the effect of persisting parent particles.

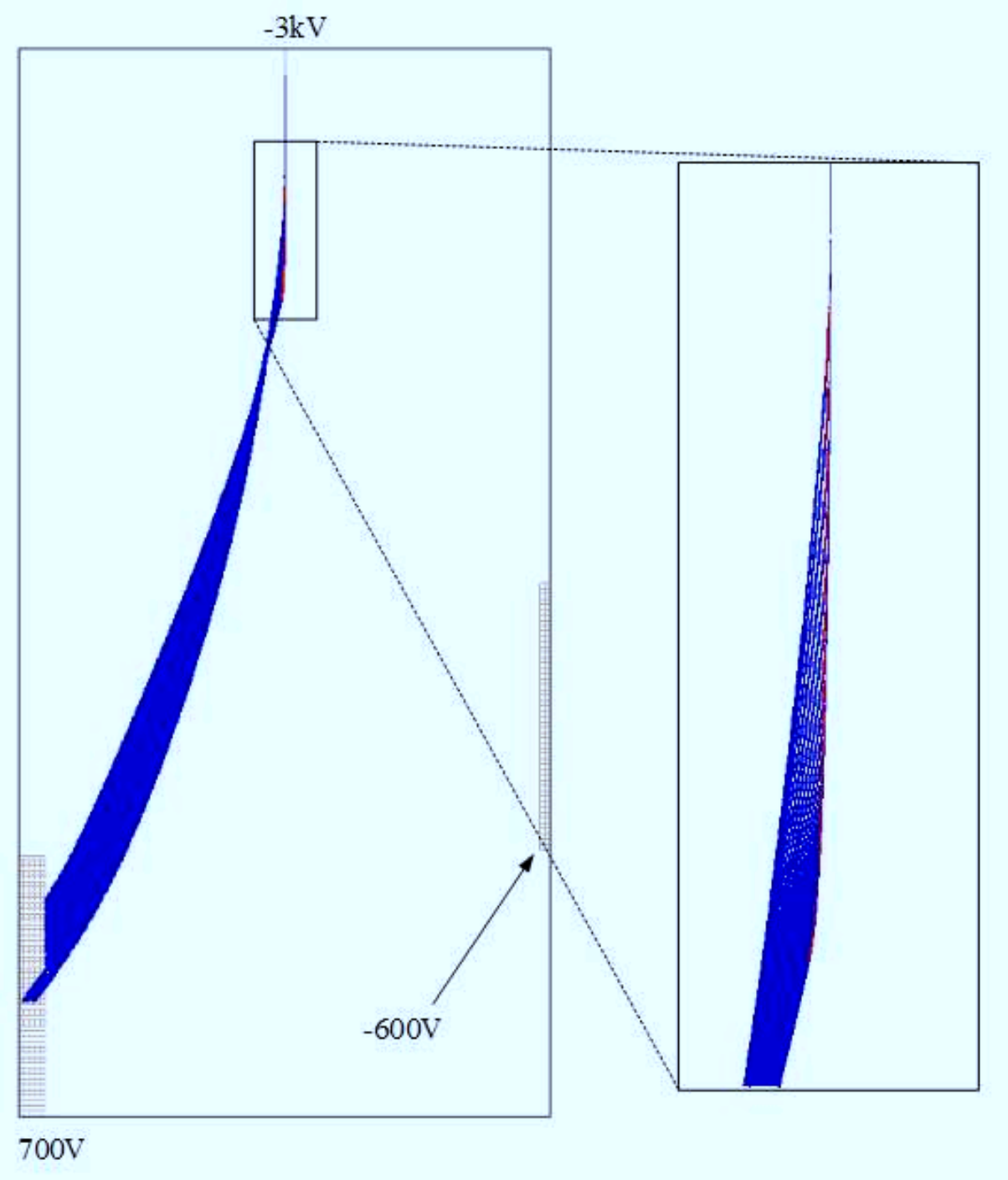


Figure 4.6: The one offspring spray with parent particles within the off-axis geometry

It can be seen that the parent particles are not correctly lensed with the same voltages on the electrodes used when they are excluded. This is due to the fact that parent particles propagate further down the system before they are light enough to be significantly affected by the plates.

This causes them to feel a greater force from the deflection plate and undershoot the orifice. It should be noted how this effect contradicts the intuition gained from the parent particle-free simulations. Parent particles lose more percent charge than percent mass resulting in child particles which start with much more charge per mass then their parent started with putting them starting closer to their own Rayleigh limit. This in turn contributes to the child particles taking less time to undergo Coulombic fission. In contrast, the parent particles will see the opposite effect, persisting longer since they start farther away from the Rayleigh limit than they did before. This persistence in parent particles also manifests itself as the neck slightly after the end of the fission events marked with red.

It should also be noted the large amount of red surpassing the total pixels imaging the trajectories. Each of these red marks represents a child particles creation. This strongly makes the case of both limiting the fission in this example to one offspring as opposed to twenty and excluding parent particles in the rest of presented simulations.

## 4.3 On-axis lens with reduction plate

The final geometry considered is an odd setup primary used in ICP-MS but under consideration by the stable isotope lab at USGS because its ”shadow block” can be used to eliminate neutrals from the spray on the directional axis. An attractive outside lens mixed with this slightly repulsive center plate allows for the charged particles to circumvent this obstacle and reach the highly charged orifice plate. The setup for this geometry is shown below in Fig. 4.7.

As with the last geometry, these voltages were determined manually and there are certainly altering solutions of voltages that will lead to ion transmission. The reduction plate is shaped as it is in ICP-MS systems and altering shapes, such as a cone, would be more beneficial should the ability to physical implement it be available. The contour map for this geometry is shown below in Fig. 4.8

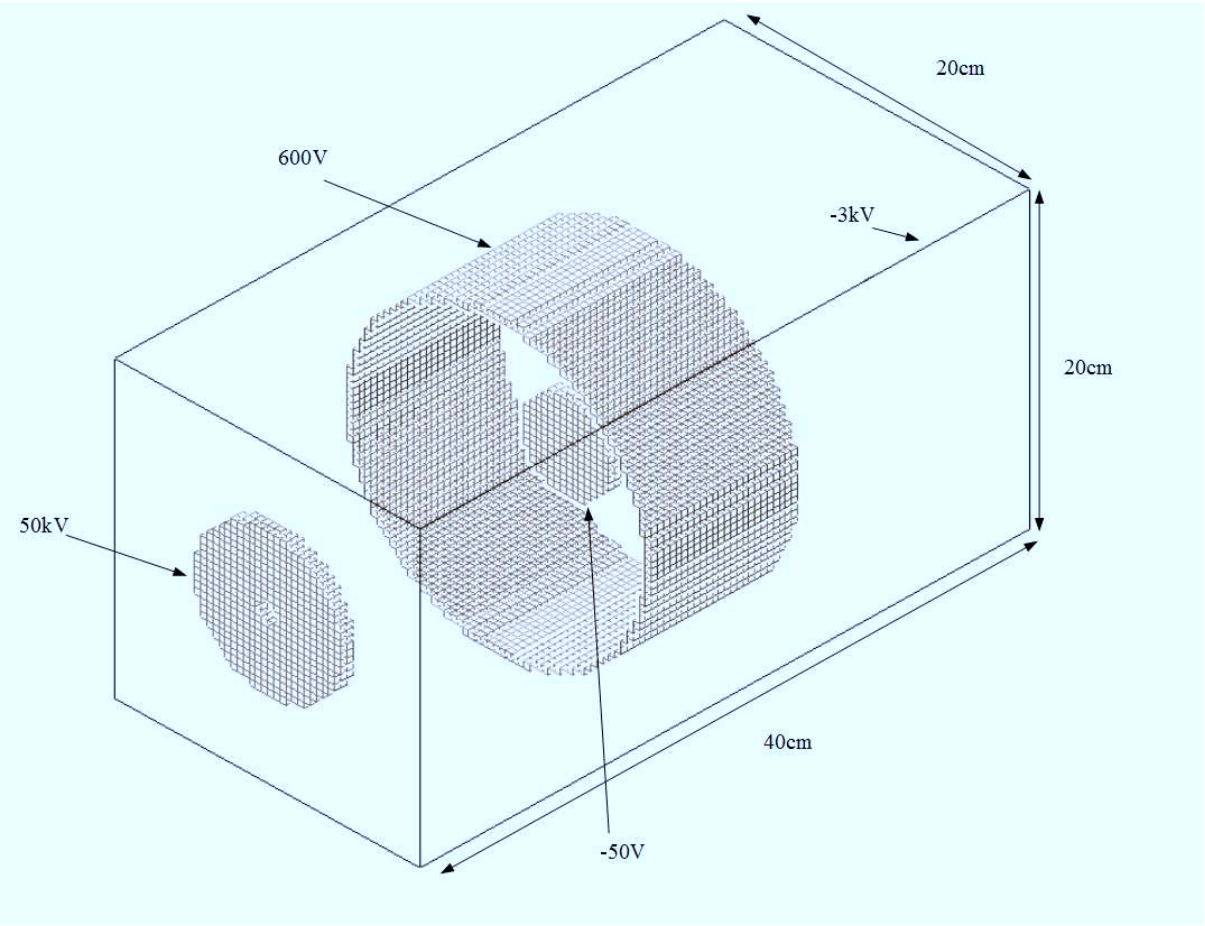


Figure 4.7: Setup for the on-axis lens with reduction plate

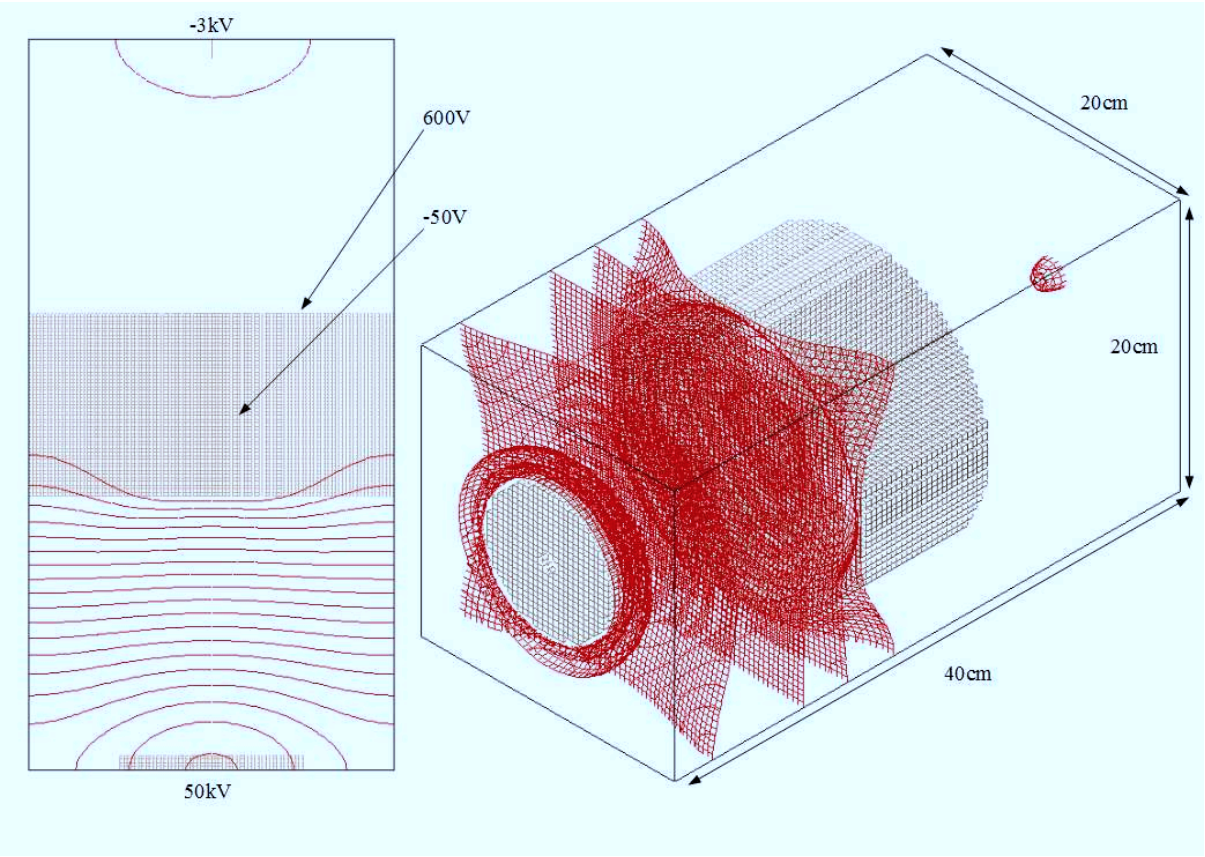


Figure 4.8: A potential contour plot for the on-axis lens with reduction plate geometry

These contours were again selected to show the regions with the largest potential gradient which is after the reduction plate. An alternate setup could be a strongly repulsive plate followed by a repulsive lens although that is made difficult with a circular plate as opposed to a cone or a sphere. The resulting simulation output for the spray is shown below in Fig. 4.9.

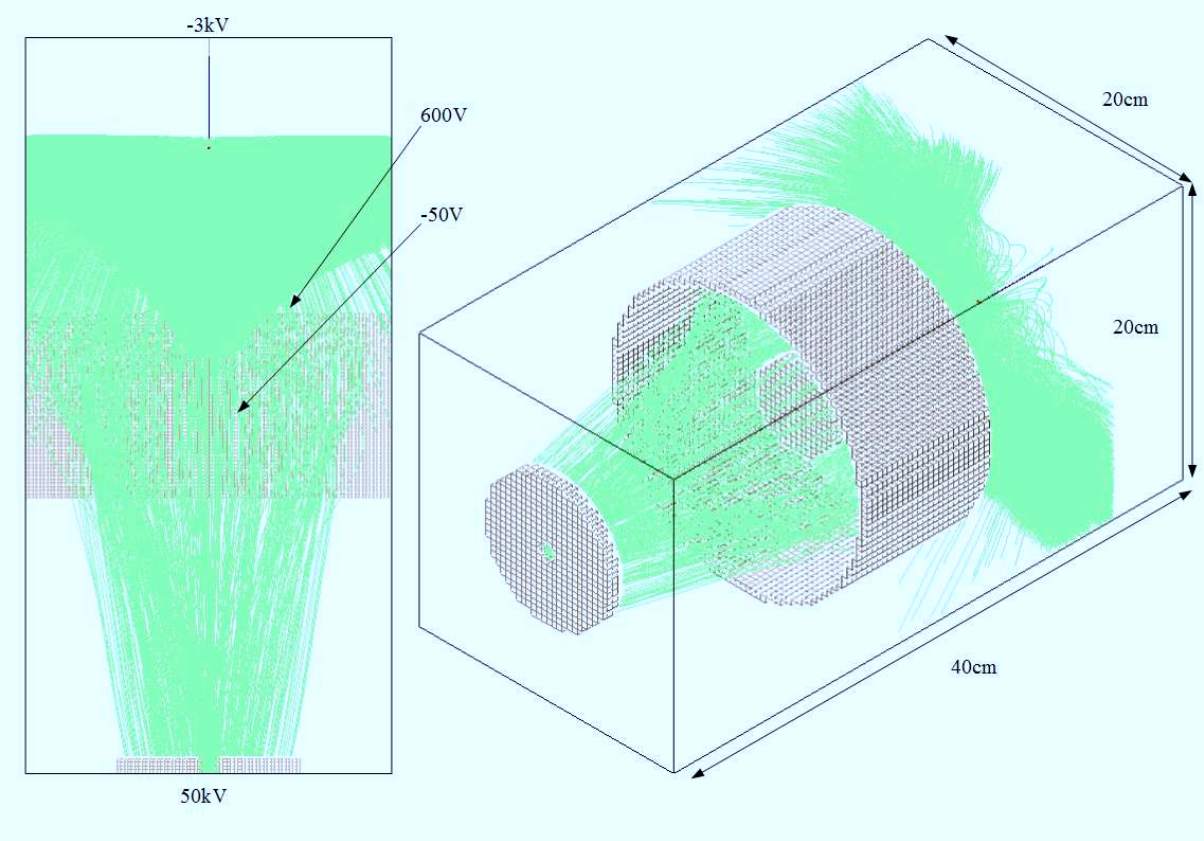


Figure 4.9: Spray simulation of the on-axis lens with reduction plate

Here can be seen a successful lensing setup yet unfortunately yields less than 0.1% of the charged particles in the system. This is further magnified by the approximation of writing out parent particles and the result in a small fraction of the actual droplet charge. This could be corrected by a more exhaustive attempt at manual voltage changing or implementation of a searching algorithm for the optimal voltage configuration. USGS will have to carefully consider this option before implementation as it may not necessarily directly transfer from the ICP-MS system and may need significant changes. Regardless, it is shown to work but low yields will be the result unless careful future analysis can be done.

Overall, the simulations are successful. It is encouraging that SIMION can handle the creation of many particles and their dynamics throughout the Coulombic fissions. The lensing of

the particles by picking voltages of the electrodes to guide them through the orifice was achieved manually and implies that a voltage finder for the highest yield electrode setup might not even be needed though in a case similar to the last one above, still could be useful.

# CHAPTER 5: CONCLUSIONS AND FUTURE STUDIES

In this thesis, simulations were presented that demonstrated the limits of the current understanding of the electrospray process. These simulations show how advantageous it would be to be able to simulate the spray prior to making a decision on instrumentation given careful knowledge of the desired system. It was shown that complex particle interactions could be successfully implemented in SIMION and that lensing the resulting collection of ions could be achieved successfully. That said, current knowledge of the theory that governs the electrospray is not comprehensive enough to create a general tool which would be useful in a laboratory setting.

These limitations of this study predominately are the empirical approximations that would be determined by better theory. These limitations include the constants that determine the thermal evaporation process at differing pressures, the insight into the Rayleigh limit that determines when a particle might undergo Coulombic fission, and the nature of child particles from a fission event. The slight limits of SIMION such as resolution of the needle, edge effects, and the need to eliminate parent particles could be resolved given enough time but the fundamental limitations in theory dissuade from perusing these studies until those questions can be answered.

Future studies along the lines of this work should be done less on the simulation side and more so on the theory. More empirical data should be acquired on the nature of child particles such that a theory might be developed. It is only after this that simulation might be able to migrate away from methanol. These types of experiments are likely currently being addressed although it may be some time until complete descriptions of the process will be available in literature. Experiments should also establish values for the condensation coefficient which determines the thermal evaporation rate as it is only known for water, ethanol, and methanol. As the condensation coefficient is an empirical patch to make up for what isn't know in theory, perhaps theoretical investigation into evaporation on the nano-scale might be a more productive pursuit as opposed to trying to find coefficients.

It is important to note that there are many groups currently investigating all of this. Primary among these questions is the difference between the charged residue model and the ion evap-

oration model mentioned in Section 2.2. More recent support for the charged residue model is continually coming to the surface and as such, the picture will become more clear on how child particles are created and characterized [40].

Regardless, SIMION has been proven to be a successful tool in analyzing the electrospray up until now and will be able to do much more in future work. Packages exist for SIMION such as "The statistical diffusion simulation" (SDS) that would help relax the requirement of a system in vacuum and would make for a natural extension for this study [41]. The SDS package combines a diffusion approach with mobility empirical data for a solvent traveling through differing pressure regimes by means of statistical mechanics and hard sphere collision approximations. A resulting smaller drift velocity from this package might explain the extra distance traveled by the initial droplet in current simulation thus allowing for not only the vacuum approximation to be relaxed, but also the need to extend the geometry past what would be a normal experimental setup size.

Another factor for future consideration in SIMION simulations is the potential problem with space charge. Space charge is the idea that at certain charge densities and current, a moving charge will see opposing charges ahead of it in the direction of its motion, creating a potential on the order of magnitude as the potential it was already moving through from other electrodes. The resulting Child-Langmuir law that describes this idea gives a maximum current that may move in a certain potential with given permittivity of the space. Whether electrosprays are candidates for this effect is a debated topic. Some sources claim it is not or they claim that the effect is so small that it does not contribute [42] but others disagree [43]. It is certainly a topic that can be explored further in SIMION.

# APPENDIX A: EXAMPLE CODE

```
simion.workbench_program()
– Code in part inspired by SIMION example code child80
– Queue of child particles to fly for current parent particle.
local child_particles =
– Scheduled value of ion_splat for next time-step (or nil if unset).
local next_ion_splat
– Whether debug print messages are enabled (1=yes,0=no)
adjustable is_debug = 1
local ion_throughput = 0 –Total ion flux from droplet
– Add a new child particle using the parameters
– in table t. Parameters can be omitted, in which case
– they default to the values of the current particle.
local function add_particle(t)
local particle =
particle.tob = t.tob or ion_time_of_birth
particle.tof = t.tof or ion_time_of_flight
particle.mass = t.mass or ion_mass
particle.charge = t.charge or ion_charge
particle.px = t.px or ion_px_mm
particle.py = t.py or ion_py_mm
particle.pz = t.pz or ion_pz_mm
particle.vx = t.vx or ion_vx_mm
particle.vy = t.vy or ion_vy_mm
particle.vz = t.vz or ion_vz_mm
particle.color = t.color or ion_color
child_particles[#child_particles+1] = particle – append
return particle end
```

```
local function target_hit(charge) –If particle has reached condition then add charge to total hit
count
ion_throughput = ion_throughput + charge
end
previoustime = 0
function segment.other_actions()
– Turn trajectory recording on (in case it was previously turned off).
sim_trajectory_image_control = 0 – YES,YES
– Handle scheduled particle terminations from previous time-step.
if next_ion_splat then
ion_splat = next_ion_splat
next_ion_splat = nil
end
if ion_splat  = 0 then – particle is terminating.
if #child_particles > 0 then – child particles exist
ion_splat = 0 – prevent termination to fly children
– Transform current particle into next scheduled child.
local data = table.remove(child_particles, 1)
–if is_debug  = 0 then print(”DEBUG: init child”, ion_number) end
ion_time_of_birth = data.tob
ion_time_of_flight = data.tof
ion_mass = data.mass
ion_charge = data.charge
ion_px_mm = data.px
ion_py_mm = data.py
ion_pz_mm = data.pz
ion_vx_mm = data.vx
ion_vy_mm = data.vy
ion_vz_mm = data.vz
```

```
ion_color = data.color
– Prevent drawing trajectory line due to manual particle movement.
sim_trajectory_image_control = 3 – NO,NO
– Add a mark at location of child particle creation.
– This is useful for both display and data recording (record on marks).
mark()
previoustime = 0
ion_time_of_flight = 0
end
end
–Determining initial conditions of droplet and calculated constants
–Constants
local eps0 = 8.854187*pow(10,-12) –Permittivity of vacuum (m-3 kg-1 s4 A2)
local rho = 0.8*pow(10,3) –(kg m-3)
local gamma = 0.02207 –Surface tension of the solvent (N m-1)
local radius = pow(ion_mass/(6.022*pow(10,26)*(4/3)*math.pi*rho),1/3)–m
stab_limit = pow((pow(ion_charge*1.60*pow(10,-19)/(8*math.pi),2)/(eps0*gamma)),(1/3)) –
Rayleigh stability limit (stab limit is 0 for most humans)
stab_limitMass = 6.022*pow(10,26)*rho*(4/3)*math.pi*pow(stab_limit,3)
–print(ion_mass .. ” mass before”)
if ion_mass > 32 then –We got to small catch
ion_mass = 6.022*pow(10,26)*(4/3)*math.pi*rho*pow(radius-1.2*pow(10,-3)*pow(10,-6)
*(ion_time_of_flight-previoustime),3) –Change mass by scale factor at each time step
previoustime = ion_time_of_flight
end
–print(ion_time_of_flight-previoustime .. ” timestep”)

–print(ion_mass .. ” mass after”)
–print(6.022*pow(10,26)*(4/3)*math.pi*pow(1.2*pow(10,-3),3)*rho*pow(10,-6)
```

```
*(ion_time_of_flight-previouststep) .. ” amount subtracted”)
–print(stab_limitMass .. ” Rayleigh limit”)
–print(ion_time_of_flight .. ”Current TOF”)
–previouststep = ion_time_of_flight
–if ion_mass > 6.022*pow(10,26)*(4/3)*math.pi*rho*pow(10*pow(10,-9),3) then –We got to small catch
if ion_mass < 0.7*stab_limitMass then –Splat is below Rayleigh stability limit (will be split later)
–if is_debug  = 0 then print(”DEBUG: new children at”, ion_px_mm) end for i = 1,20 do add_particlemass = 0.0025*ion_mass, charge = 0.01*ion_charge, vx = ion_vx_mm + 0.05*(rand()-0.5), vy = ion_vy_mm + 0.05*(rand()-0.5), vz = ion_vz_mm, color = ion_color+1
–splat at start of next time-step (not this one)
next_ion_splat = -2 – dead in water
end
–add_particlemass = 0.095*ion_mass, charge = 0.08*ion_charge
end –end
if (ion_px_mm < 10 and ion_px_mm > 0 and ion_py_mm < 105 and ion_py_mm > 95 and ion_pz_mm < 355 and ion_pz_mm > 345) then –Determining if target has been reached target_hit(ion_charge)
next_ion_splat = -2
end
max_time = ion_time_of_flight –Recording maxflight time
end
function segment.terminate()
print(ion_throughput)
end
```

# REFERENCES


[1] E. Butter. N. n. greenwood, a. earnshaw: Chemistry of the elements. *Crystal Research and Technology*, 20(5):662–662, 1985. ISSN 1521-4079. doi: 10.1002/crat.2170200510. URL http://dx.doi.org/10.1002/crat.2170200510.

[2] R.T. Morrison and R.N. Boyd. *Study Guide to Organic Chemistry*. Allyn and Bacon, 1987. URL https://books.google.com/books?id=f-ZhmgEACAAJ.

[3] Fathi Habashi. *Kinetics and mechanism of gold and silver dissolution in cyanide solution*. Montana College of Mineral Science and Technology, 1967.

[4] Moran R. Straskrabra V. Environmental occurrence and impacts of arsenic at gold mining sites in the western united states. *International Mines Water Association*, pages 181–191, 2006.

[5] Goldindo. Mulatos gold mine mexico. *Largest Gold Mines In The World I Gold Mines Around The World I Gold And Silver Mining I World Mining News I Gold Mines In World*, 2015. URL https://goldindo.wordpress.com/2015/11/29/mulatos-gold-mine-mexico/.

[6] William J. Boecklen, Christopher T. Yarnes, Bethany A. Cook, and Avis C. James. On the use of stable isotopes in trophic ecology. *Annual Review of Ecology, Evolution, and Systematics*, 42(1):411–440, 2011. doi: 10.1146/annurev-ecolsys-102209-144726. URL http://dx.doi.org/10.1146/annurev-ecolsys-102209-144726.

[7] J. R. Arnold and W. F. Libby. Age determinations by radiocarbon content: Checks with samples of known age. *Science*, 110(2869):678–680, 1949. doi: 10.1126/science.110.2869.678. URL http://www.sciencemag.org/content/110/2869/678.short.

[8] *Stable Isotopes in Ecology and Environmental Science*. Blackwell Publishing Ltd, 2008. doi: 10.1002/9780470691854.fmatter.

[9] Michael A. Poage and C. Page Chamberlain. Empirical relationships between elevation and the stable isotope composition of precipitation and surface waters: Considerations for studies of paleoelevation change. *American Journal of Science*, 301(1):1–15, 2001. doi: 10.2475/ajs.301.1.1. URL http://www.ajsonline.org/content/301/1/1.abstract.

[10] R.B. Cole. *Electrospray Ionization Mass Spectrometry: Fundamentals, Instrumentation, and Applications*. John Wiley and Sons, Ltd., first edition, 1997.

[11] Electrospray ionisation, 2016. URL http://www.mpibpc.mpg.de/107942/gallery.

[12] USA. National Institute of Standards and Technology. *NIST Chemistry Webbook*. U.S. Secretary of Commerce, 2003. URL https://books.google.com/books?id=NWKBQwAACAAJ.

[13] Lekha Sleno and Dietrich A. Volmer. Ion activation methods for tandem mass spectrometry. *Journal of Mass Spectrometry*, 39(10):1091–1112, 2004. ISSN 1096-9888. doi: 10.1002/jms.703. URL http://dx.doi.org/10.1002/jms.703.

[14] The nobel prize in chemistry 2002, 2014. URL http://www.nobelprize.org/nobel_prizes/chemistry/laureates/2002/.

[15] J. J. Pitt. Principles and applications of liquid chromatography-mass spectrometry in clinical biochemistry. *Clin Biochem Rev*, 30(1):19–34, Feb 2009.

[16] Mazumdar S. Banerjee S. Electrospray ionization mass spectrometry: A technique to access the information beyond the moleculr weight of the analyte. *International Journal of Analytical Chemistry*, 2012(40), 2012.

[17] J. P. Whitelegge, J. le Coutre, J. C. Lee, C. K. Engel, G. G. Privé, K. F. Faull, and H. R. Kaback. Toward the bilayer proteome, electrospray ionization-mass spectrometry of large, intact transmembrane proteins. *Proceedings of the National Academy of Sciences*, 96(19): 10695–10698, 1999. doi: 10.1073/pnas.96.19.10695.

[18] M. Pauly, M. Sroka, J. Reiss, G. Rinke, A. Albarghash, R. Vogelgesang, H. Hahne, B. Kuster, J. Sesterhenn, K. Kern, and S. Rauschenbach. A hydrodynamically optimized nano-electrospray ionization source and vacuum interface. *Analyst*, 139:1856–1867, 2014. doi: 10.1039/C3AN01836A. URL http://dx.doi.org/10.1039/C3AN01836A.

[19] Jason S. Page, Ryan T. Kelly, Keqi Tang, and Richard D. Smith. Ionization and transmission efficiency in an electrospray ionization-mass spectrometry interface. *Journal of the American Society for Mass Spectrometry*, 18(9):1582 – 1590, 2007. ISSN 1044-0305. doi: http://dx.doi.org/10.1016/j.jasms.2007.05.018. URL http://www.sciencedirect.com/science/article/pii/S1044030507004357.

[20] Eric Janusson, Amelia V. Hesketh, Karlee L. Bamford, Katherine Hatlelid, Rehan Higgins, and J. Scott McIndoe. Spatial effects on electrospray ionization response. *International Journal of Mass Spectrometry*, 388:1 – 8, 2015. ISSN 1387-3806. doi: http://dx.doi.org/10.1016/j.ijms.2015.07.016. URL http://www.sciencedirect.com/science/article/pii/S1387380615002195.

[21] JonathanT. Cox, Ioan Marginean, RichardD. Smith, and Keqi Tang. On the ionization and ion transmission efficiencies of different esi-ms interfaces. *Journal of The American Society for Mass Spectrometry*, 26(1):55–62, 2015. ISSN 1044-0305. doi: 10.1007/s13361-014-0998-5. URL http://dx.doi.org/10.1007/s13361-014-0998-5.

[22] Pfeifer J Hendricks C. Parametric studies of electrohydrodynamic spraying. *AIAA*, 6(3): 496–502, 1968.

[23] L. B. Loeb, A. F. Kip, G. G. Hudson, and W. H. Bennett. Pulses in negative point-to-plane corona. *Phys. Rev.*, 60:714–722, Nov 1941. doi: 10.1103/PhysRev.60.714. URL http://link.aps.org/doi/10.1103/PhysRev.60.714.

[24] Lord Rayleigh. volume 14. Philos. Mag., 1882.

[25] C. N. Davis. *In Fundamentals of Aerosol Science*. Wiley: New York, 1978.

[26] Paul Kebarle and Liang Tang. From ions in solution to ions in the gas phase - the mechanism of electrospray mass spectrometry. *Analytical Chemistry*, 65(22):972A–986A, 1993. doi: 10.1021/ac00070a001. URL http://dx.doi.org/10.1021/ac00070a001.

[27] Alessandro Gomez and Keqi Tang. Charge and fission of droplets in electrostatic sprays. *Physics of Fluids*, 6(1):404–414, 1994. doi: http://dx.doi.org/10.1063/1.868037. URL http://scitation.aip.org/content/aip/journal/pof2/6/1/10.1063/1.868037.

[28] Daniel C. Taflin, Timothy L. Ward, and E. James Davis. Electrified droplet fission and the rayleigh limit. *Langmuir*, 5(2):376–384, 1989. doi: 10.1021/la00086a016. URL http://dx.doi.org/10.1021/la00086a016.

[29] I. Aguirre de Carcer and J.FernÃ¡ndez de la Mora. Effect of background gas on the current emitted from taylor cones. *Journal of Colloid and Interface Science*, 171(2):512 – 517, 1995. ISSN 0021-9797. doi: http://dx.doi.org/10.1006/jcis.1995.1210. URL http://www.sciencedirect.com/science/article/pii/S0021979785712106.

[30] Sheriff Falana Aziza and Consta Styliani. Charge-induced instabilities of droplets containing macromolecular complexes. *Canadian Journal of Chemistry*, 93(2):173–180, 2015. doi: 10.1139/cjc-2014-0299. URL http://dx.doi.org/10.1139/cjc-2014-0299.

[31] J. V. Iribarne and B. A. Thomson. On the evaporation of small ions from charged droplets. *The Journal of Chemical Physics*, 64(6):2287–2294, 1976. doi: http://dx.doi.org/10.1063/1.432536. URL http://scitation.aip.org/content/aip/journal/jcp/64/6/10.1063/1.432536.

[32] B. A. Thomson and J. V. Iribarne. Field induced ion evaporation from liquid surfaces at atmospheric pressure. *The Journal of Chemical Physics*, 71(11):4451–4463, 1979. doi: http://dx.doi.org/10.1063/1.438198. URL http://scitation.aip.org/content/aip/journal/jcp/71/11/10.1063/1.438198.

[33] D.A. Manura D.J., Dahl. *SIMION Version 8.0 User Manual*. Scientific Instrument Services, Inc., 2008.

[34] Bradley B. Schneider, D. J. Douglas, and David D. Y. Chen. An atmospheric pressure ion lens to improve electrospray ionization at low solution flow-rates. *Rapid Communications in Mass Spectrometry*, 15(22):2168–2175, 2001. ISSN 1097-0231. doi: 10.1002/rcm.481. URL http://dx.doi.org/10.1002/rcm.481.

[35] Bradley B Schneider, D.J Douglas, and David D.Y Chen. An atmospheric pressure ion lens that improves nebulizer assisted electrospray ion sources. *Journal of the American Society for Mass Spectrometry*, 13(8):906 – 913, 2002. ISSN 1044-0305. doi: http://dx.doi.org/10.1016/S1044-0305(02)00389-6. URL http://www.sciencedirect.com/science/article/pii/S1044030502003896.

[36] E.E. Gulcicek and C.M. Whitehouse. Ion focusing lensing system for a mass spectrometer interfaced to an atmospheric pressure ion source, July 11 1995. URL http://www.google.com/patents/US5432343. US Patent 5,432,343.

[37] C.W. Russ, S.M. Fischer, and R.K. Crawford. Atmospheric pressure ion source high pass ion filter, September 26 2006. URL http://www.google.ba/patents/US7112786. US Patent 7,112,786.

[38] Ph.D. Ruth E. Wolf. What is icp-ms? ... and more importantly, what can it do?, 2016. URL http://crustal.usgs.gov/laboratories/icpms/intro.html.

[39] Liang Tang and Paul Kebarle. Dependence of ion intensity in electrospray mass spectrometry on the concentration of the analytes in the electrosprayed solution. *Analytical Chemistry*, 65(24):3654–3668, 1993. doi: 10.1021/ac00072a020. URL http://dx.doi.org/10.1021/ac00072a020.

[40] Lars Konermann, Robert G. McAllister, and Haidy Metwally. Molecular dynamics simulations of the electrospray process: Formation of nacl clusters via the charged residue mechanism. *The Journal of Physical Chemistry B*, 118(41):12025–12033, 2014. doi: 10.1021/jp507635y. URL http://dx.doi.org/10.1021/jp507635y. PMID: 25242574.

[41] Anthony D. Appelhans and David A. Dahl. Simion ion optics simulations at atmospheric pressure. *International Journal of Mass Spectrometry*, 244(1):1 – 14, 2005. ISSN 1387-3806. doi: http://dx.doi.org/10.1016/j.ijms.2005.03.010. URL http://www.sciencedirect.com/science/article/pii/S1387380605001089.

[42] Teruyuki Nagamune Isao Endo. *Nano/Micro Biotechnology*. Springer-Verlag Berlin Heidelberg, 1st edition, 2010. doi: 10.1007/978-3-642-14947-4.

[43] P. Mirbod S. Gallucci. Comsol multiphysics software used as a laplacian potential simulator for an electrospray propulsion system extraction region.